

A Free Lunch with Influence Functions? Improving Neural Network Estimates with Concepts from Semiparametric Statistics

Matthew J. Vowels

m.j.vowels@surrey.ac.uk

CVSSP

University of Surrey, United Kingdom

Sina Akbari

sina.akbari@epfl.ch

BAN

EPFL, Lausanne, Switzerland

Jalal Etesami

seyed.etesami@epfl.ch

BAN

EPFL, Lausanne, Switzerland

Necati Cihan Camgoz

n.camgoz@surrey.ac.uk

CVSSP

University of Surrey, United Kingdom

Richard Bowden

r.bowden@surrey.ac.uk

CVSSP

University of Surrey, United Kingdom

Abstract

Parameter estimation in the empirical fields is usually undertaken using parametric models, and such models are convenient because they readily facilitate statistical inference. Unfortunately, they are unlikely to have a sufficiently flexible functional form to be able to adequately model real-world phenomena, and their usage may therefore result in biased estimates and invalid inference. Unfortunately, whilst non-parametric machine learning models may provide the needed flexibility to adapt to the complexity of real-world phenomena, they do not readily facilitate statistical inference, and may still exhibit residual bias. We explore the potential for semiparametric theory (in particular, the Influence Function) to be used to improve neural networks and machine learning algorithms in terms of (a) improving initial estimates without needing more data (b) increasing the robustness of our models, and (c) yielding confidence intervals for statistical inference. We propose a new neural network method ‘MultiNet’, which seeks the flexibility and diversity of an ensemble using a single architecture. Results on causal inference tasks indicate that MultiNet yields better performance than other approaches, and that all considered methods are amenable to improvement from semiparametric techniques under certain conditions. In other words, with these techniques we show that we can improve existing

neural networks for ‘free’, without needing more data, and without needing to retrain them. Finally, we provide the expression for deriving influence functions for estimands from a general graph, and the code to do so automatically.

1. Introduction

Most methods being utilized in empirical fields such as psychology or epidemiology are parametric models [6, 65], which are convenient because they facilitate statistical inference and the acquisition of confidence intervals (e.g. for purposes of null hypothesis testing). Indeed, being able to perform statistical tests and reliably quantify uncertainty is especially important when evaluating the efficacy of treatments or interventions. One approach to perform such tests is by assuming parametric model (e.g. linear model) for the underlying generating mechanism. However, it has been argued that linear models are incapable of modeling most realistic data generating processes and that we should instead be using modern machine learning techniques [64–66, 71]. Unfortunately, most machine learning models are non-parametric and do not readily facilitate statistical inference. Furthermore, even though machine learning algorithms are more flexible, they are still likely to be biased because they are not targeted to the specific parameter of interest [65]. So, what can we do?

By leveraging concepts from the field of semiparametric statistics, we can begin to address these issues. Indeed, by combining elements of semiparametric theory with machine learning methods, we can enjoy the best of both worlds: We can avoid having to make unreasonably restrictive assumptions about the underlying generative process, and can nonetheless undertake valid statistical inference. Furthermore, we can also leverage an estimator update process to achieve greater precision in existing estimators, without needing to retrain the network, and without needing any additional data [5, 62, 65], a so-called ‘free lunch’ [73].¹

One example of an existing method which combines machine learning and semiparametric theory is targeted learning [65, 66].² Unfortunately, this technique, and many related techniques involving influence functions (IFs) and semiparametric theory, have primarily been popularized outside the field of machine learning. In parallel, machine learning has focused on the development equivalent methods using deep neural network (NN) methods for causal inference (see *e.g.*, [4, 11, 12, 42, 56, 74, 78]), which may exhibit residual bias. As such, many of the principles and theory associated with semiparametrics and IFs are underused and underappreciated within the machine learning community, and it remains unknown to what extent these techniques can be applied to NN based estimators.

More generally, and in spite of a large body of work describing the theoretical properties of semiparametric methods for estimation outside of machine learning, there has been little empirical comparison of techniques like targeted learning against those considered state of the art at the intersection of machine learning and causal inference. In particular, there now exist numerous NN based methods, and practitioners may find themselves choosing between the alluring ‘deep learning’ based methods and those which perhaps, rightly or wrongly, have less associated hype. Such a comparison is therefore extremely important, especially given that a theoretical framework for establishing the statistical guarantees of NNs is yet elusive [10].

Specifically, we explore the potential for semiparametric techniques, in particular, various applications of IFs, to (a) improve the accuracy of estimators by ‘de-biasing’ them, (b) yield estimators which are more robust to model misspecification (double-robustness), and (c) derive confidence intervals for valid statistical inference. Our motivating application example is chosen but not limited to be the estimation of the causal effect of a treatment or intervention on an outcome from observational data. It is possible to adapt the techniques for use in computer vision [37] and NLP [26].

Finally, experiments highlight that even for simple datasets, NNs do not yield estimators close enough to be

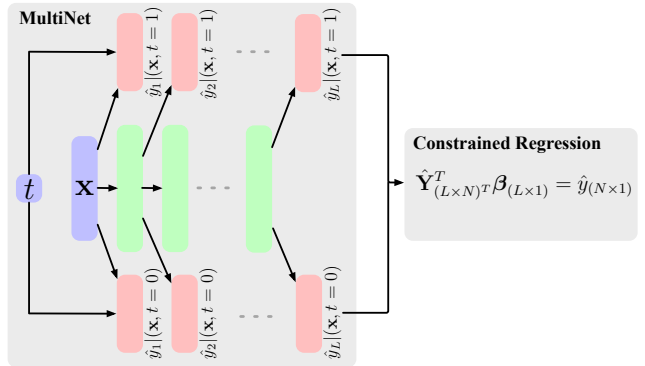


Figure 1. Block diagram for MultiNet. At each layer $l = \{1, \dots, L\}$ of the network, the outcome y is estimated using covariates \mathbf{x} (which can include treatment t). The treatment is used to select between two estimation arms. Once the network has been trained, the outcomes from each layer are combined and a weighted regression is performed. The weights β in the regression are constrained to be positive and sum to 1. An equivalent single-headed network can be used for the treatment model $\hat{t}|\mathbf{x}$.

amenable to improvement via IFs (as we will discuss below, the assumption is that the bias of the initial estimator can be approximated as a linear perturbation). We therefore propose a new NN pseudo-ensemble method ‘MultiNet’ with constrained weighted averaging (see Fig. 1) as a means to adapt to datasets with differing levels of complexity, in a similar way to the Super Learner ensemble approach [63], which is popular in epidemiology.

In summary, we wish to answer the following questions: (1) Can NNs be improved using the one-step, submodel, or targeted regularization approaches? (2) How do NN methods compare against other estimators, with and without IF update techniques? And (3) Can we adapt a NN such that its performance more closely resembles that of an ensemble of diverse models? The associated contributions of this paper are therefore:

- A top-level introduction to the basics behind semiparametric theory and influence functions.
- A comparison of the estimation performance of NNs and other algorithms with and without semiparametric techniques (variants on Targeted Learning approaches)
- A new method ‘MultiNet’ which attempts to mimic the performance of an ensemble with a single NN
- An expression for deriving influence functions for estimands from a general causal graph, and the code to do so automatically.³

¹The term ‘free lunch’ is a reference to the adage of unknown origin (but probably North American) ‘there ain’t no such thing as a free lunch’.

²For an overview of some other related methods see [10].

³Code for models, experiments, and IF derivation is accessible here: https://github.com/matthewvowels1/semiparametrics_and_NNs_release/.

We evaluate causal inference task performance in terms of (a) precision in estimation (and the degree to which we can achieve debiasing), (b) double robustness, and (c) normality and statistical inference. We find that NNs are outperformed by conventional ensemble based methods, but that they are nonetheless amenable to improvement via the use of semiparametric techniques when combined with an alternative ensemble method (the free lunch). We find our MultiNet flexibly adapts to the complexity of the problem, and provides the best performance across datasets. We confirm that all methods benefit from the application of the semiparametric techniques, in particular in realising a normally distributed outcome directly amenable to statistical inference.

The paper is structured as follows: We begin by reviewing previous work in Sec. 2 and provide background theory on the motivating case of estimating causal effects from observational data in Sec. 3. We then provide a top level introduction to influence functions, how to use them to debias our estimators, and a discussion of open questions in Sec. 3.1-3.4. MultiNet is presented in Sec. 4. Our evaluation methodology is described in Sec. 5 and we present and discuss results in Sec. 6. Finally, we provide a summary of the experiments, limitations, and opportunities for further work in Sec. 7.

2. Previous Work

The possible applications of semiparametrics in machine learning are broad and under-explored, but IFs in particular have only seen sporadic application in explainability for computer vision [37] and NLP [26] models, causal model selection [1] and uncertainty quantification for deep learning [2]. Outside of machine learning, in particular in the fields of epidemiology and econometrics, semiparametric methods are becoming more popular, and include targeted learning [65] and double machine learning [9]. In statistics, alternatives have been developed which include doubly robust conditional ATE estimation [36] and IF-learning [10].

However, within the field representing the confluence of causal inference and machine learning, the focus seems to have been on the development of NN methods (see CEVAE [42], CFR-Net [56], GANITE [78], Intact-VAE [75] etc.), without a consideration for statistical inference or semiparametric theory [11, 12]. Indeed, to the best of our knowledge, the application of semiparametric theory to debias NNs has only be used twice in the field representing the confluence of machine learning and causal inference. Firstly, in DragonNet [58], a method designed for ATE estimation, and secondly in TVAE [72], a variational, latent variable method for conditional ATE and ATE estimation. Both methods incorporate targeted regularization, but do not readily yield statistical inference because to do so requires asymptotic normality (and this is not evaluated in the studies) as well

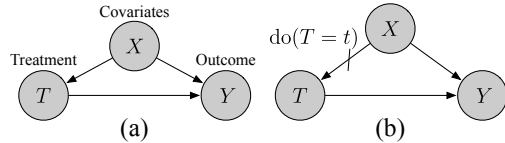


Figure 2. Directed Acyclic Graphs (DAGs) for estimating the effect of treatment $T = t$ on outcome Y with confounding X .

as explicit evaluation of the IF.

Finally, other comparisons of the performance of semiparametric approaches exist. For example, the robustness of targeted learning approaches to causal inference on nutrition trial data [41] includes a very useful summary table of previous findings and includes its own evaluations. However, it does not include comparisons with NN-based learners, and seeks the answers to different questions relevant to practitioners in the empirical fields. Another example evaluation was undertaken by [43] but has a didactic focus.

3. Causal Inference and Influence Functions

3.1. Causal Inference

The concepts in this paper are applicable to estimation tasks in general, but we focus on the specific task of estimating a causal effect, which is of the upmost importance for policy making [38], the development of medical treatments [49], the evaluation of evidence within legal frameworks [45, 59], and others. A canonical characterization of the problem of causal inference from observational data is depicted in the Directed Acyclic Graphs (DAGs) shown in Figs. 2, and we provide an overview of causal inference in this section. We also provide further information in the supplementary, and point interested readers towards accessible overviews by [23, 47, 70].

We use $\mathbf{x}_i \sim p(\mathbf{x}) \in \mathbb{R}^m$ to represent the m -dimensional, pre-treatment covariates for individual i assigned factual treatment $t_i \sim p(t|\mathbf{x}) \in \{0, 1\}$ resulting in outcome $y_i \sim p(y|\mathbf{x}, t)$. Together, these constitute dataset $\mathcal{D} = \{[y_i, t_i, \mathbf{x}_i]\}_{i=1}^n$ sampled from $\mathcal{P} = \{Y, T, X\}$ where n is the sample size.

Fig. 2 (a) is characteristic of observational data, where the assignment of treatment is related to the covariates. One of the most common causal estimands is the Average Treatment Effect (ATE): $\tau(\mathbf{x}) = \mathbb{E}_{\mathbf{x}}[\mathbb{E}[y(1)|\mathbf{x}] - \mathbb{E}[y(0)|\mathbf{x}]]$. Here, $y(1)$ and $y(0)$ are what are known as *potential outcomes* for the outcome under treatment and the outcome under no treatment, respectively [32]. In practice, we only have access to one of these two quantities, whilst the other is missing. Using *do*-calculus [46] we can establish whether, under a number of strong assumptions⁴, the desired causal

⁴These assumptions are the Stable Unit Treatment Value Assumption (SUTVA), Positivity, and Ignorability/Unconfoundedness - see supple-

estimand can be expressed in terms of the observed joint distribution, and thus whether the effect is *identifiable*. For the graph in Fig. 2 (a), the outcome under intervention is identifiable and can be expressed as:

$$P(y|\text{do}(t = t^*)) = \int_{\mathbf{x}} P(y|\mathbf{x}, t^*)P(\mathbf{x}), \quad (1)$$

which is estimable from observational data. Here, t^* is the specific intervention of interest (e.g., $t^* = 1$). One may use a regression to approximate the integral in Eq. (1), and plug-in estimators \hat{Q} (e.g., NNs) can be used for estimating the ATE as:

$$\hat{\tau}(\hat{Q}; \mathbf{x}) = \frac{1}{n} \sum_{i=1}^n (\hat{Q}(1, \mathbf{x}_i) - \hat{Q}(0, \mathbf{x}_i)), \quad (2)$$

We use the hat notation to designate an estimated (rather than true population) quantity. In the simplest case, we may use a linear or logistic regression, depending on whether the outcome is continuous or binary. Unfortunately, if one imagines the true joint distribution to fall somewhere within an infinite set of possible distributions, we deliberately handicap ourselves by using a family of linear models because such a family is unlikely to contain the truth. The consequences of such model misspecification can be severe, and results in biased estimates [71]. In other words, no matter how much data we collect, our estimate will converge to the wrong quantity, necessarily resulting in a false positive rate which converges to 100%. Furthermore, even with correct specification of our plug-in estimators, our models are unlikely to be ‘targeted’ to the desired estimand, because they often estimate quantities superfluous to the estimand but necessary for the plug-in estimator (e.g., other relevant factors or statistics of the joint distribution). As a result, in many cases there exist opportunities to reduce residual bias using what are known as *influence functions*.

3.2. Influence Functions

Semiparametric theory and, in particular, the concept of Influence Functions (IFs), are known to be challenging to assimilate [18, 28, 40]. Here we attempt to provide a brief, top-level intuition, but a detailed exposition lies beyond the scope of this paper (more details are included in the supplementary). Interested readers are encouraged to consider introductions by [18, 28, 35, 62].

An estimator $\Psi(\hat{\mathcal{P}}_n)$ for an estimand $\Psi(\mathcal{P})$ (for example, the ATE) has an IF, ϕ , if it can be expressed as follows:

$$\sqrt{n}(\Psi(\hat{\mathcal{P}}_n) - \Psi(\mathcal{P})) = \frac{1}{\sqrt{n}} \sum_{i=1}^n \phi(Z_i, \mathcal{P}) + o_p(1), \quad (3)$$

mentary for more information.

where Z_i is a sample from the true distribution \mathcal{P} , $\hat{\mathcal{P}}_n$ is the empirical distribution or, alternatively, a model of some part thereof (e.g., a predictive distribution parameterized by a NN), $o_p(1)$ is an error term that converges in probability to zero, and ϕ is a function with a mean of zero and finite variance [62, pp.21]. This tells us that the difference between the true quantity and the estimated quantity can be represented as the sum of a bias term and some error term which converges in probability to zero. The IF itself is a function which models how much our estimate deviates from the true estimand, up to an error term. If an estimator can be written in terms of its IF, then by central limit theorem and Slutsky’s theorem, we have that Eq. (3) converges in distribution to a normal distribution with mean zero and variance equal to the variance of the IF. This is a key result that enables us to derive confidence intervals and perform inference.

One of the original introductions of IFs concerned their use in robust statistics for evaluating how sensitive an estimator is to changes in the sample distribution [25]. However, our intended use is different to this, because we wish to use them to derive unbiased estimators without needing additional data, and to derive confidence intervals without needing to bootstrap. The next key result is related to the Riesz Representation Theorem [19, 52] (see supplementary), and enables us to express ϕ in Eq. (3) as:

$$\frac{1}{n} \sum_{i=1}^n \phi(Z_i, \mathcal{P}) = \left. \frac{d\Psi(\epsilon\hat{\mathcal{P}}_n + (1-\epsilon)\mathcal{P})}{d\epsilon} \right|_{\epsilon=0}. \quad (4)$$

Here, $\frac{d\Psi}{d\epsilon}$ is the pathwise functional derivative of the target estimand with respect to ϵ which parameterizes a linear perturbation of the true distribution (which is our observational distribution). The argument to Ψ in the numerator of Eq. (4) parameterizes a linear path towards the true distribution, which occurs when $\epsilon = 0$. The analytic expression for Eq. (4) is evaluated at distribution \mathcal{P} when $\epsilon = 0$, but we can alternatively evaluate it at the empirical distribution $\hat{\mathcal{P}}_n$ (when $\epsilon = 1$). Doing so introduces a negative sign (because we are evaluating the pathwise derivative in the opposite direction) which is absorbed when we substitute it into Eq. (3), and allows us to estimate the true estimand in terms of empirical quantities. This yields:

$$\Psi(\mathcal{P}) = \Psi(\hat{\mathcal{P}}_n) + \frac{1}{n} \sum_{i=1}^n \phi(Z_i, \hat{\mathcal{P}}_n) + o_p(1/\sqrt{n}), \quad (5)$$

where now Z_i is drawn from $\hat{\mathcal{P}}_n$. Eq. (5) is a Von Mises Expansion (VME), which is the functional analogue of the Taylor expansion. In essence, we are representing our estimate $\Psi(\hat{\mathcal{P}}_n)$ as lying on a path to the true estimand, the direction of which is represented by the pathwise derivative of this estimand with respect to the amount of perturbation.

3.3. Updating/Debiasing our Estimators with IFs

If we can estimate the IF ϕ then we can update our initial estimator $\Psi(\hat{\mathcal{P}}_n)$ according to Eq. (5) in order to reduce the residual bias which the IF is essentially modeling. To be clear, this means we can improve our initial NN estimators, without needing more data, and obtain a so called ‘free lunch’. We consider three ways to leverage the IF to reduce bias which we refer to as (1) the one-step update, (2) the submodel update (sometimes referred to as a targeted update), and (3) targeted regularization. The first two approaches can be trivially applied to estimators which have already been trained, making them attractive as post-processing methods for improving estimation across different application areas.

To better illustrate these approaches, we consider the ATE to be our chosen target estimand, the IF for which is derived in [28] as well as supplementary and is given below. For this derivation, we assume $t = t^* \in \{0, 1\}$ such that the target estimand becomes the potential outcome under intervention $t = t^*$: $\Psi(\mathcal{P}) = \mathbb{E}_Y[\mathbb{E}_X[Y|T = t, X]]$ for each t considered separately:

$$\phi(Z, \hat{\mathcal{P}}_n) = \frac{\delta(t)}{f(t|\tilde{\mathbf{x}})} (\tilde{y} - \mathbb{E}[y|t, \tilde{\mathbf{x}}]) + \mathbb{E}[y|t, \tilde{\mathbf{x}}] - \Psi(\hat{\mathcal{P}}_n). \quad (6)$$

Here, the $Z = (X, T, Y)$, \tilde{y} and $\tilde{\mathbf{x}}$ are samples from our empirical distribution, δ is the delta function (which for discrete t acts like an indicator function) and t is set according to the treatment we wish to evaluate. We need plug-in estimators $\pi(\tilde{\mathbf{x}}) \approx f(t|\tilde{\mathbf{x}})$ (propensity score / treatment model), and $m(t, \tilde{\mathbf{x}}) \approx \mathbb{E}[Y|t, \tilde{\mathbf{x}}]$ (outcome model).

One-Step and Submodel Approach: Using the first, *one-step* approach, the original estimator $\Psi(\hat{\mathcal{P}}_n)$ can be improved by a straightforward application of the VME Eq. (5) - one takes the initial estimate and adds to it the estimate of the IF to yield an estimate which accounts for the ‘plug-in bias’. In the case of the ATE, the IF which is given in Eq. (6), this yields the augmented inverse propensity weighted (AIPW) estimator [28, 39, 44].

The second *submodel* approach updates the initial estimate by solving $\sum_{i=1}^n \phi(Z_i, \hat{\mathcal{P}}_n) = 0$. This approach works by first constructing a parametric submodel in terms of the propensity score nuisance parameter, and removes the associated bias according to:

$$m(t, \tilde{\mathbf{x}})^* = m(t, \tilde{\mathbf{x}}) + \hat{\gamma}H(Z_i). \quad (7)$$

Here, $H(Z_i) = \delta(t)/f(t|\tilde{\mathbf{x}})$ (which appears in Eq. (6)), and is known as the clever covariate. The parameter $\hat{\gamma}$ is estimated as the coefficient in the associated intercept-free linear regression. Both procedures solve what is known as the *efficient influence function*, and following the update,

the residual bias will be zero. In practice, the two methods yield different results with finite samples. In particular, the one-step / AIPW estimator may yield estimates outside of the range of values allowed according to the parameter space, and be more sensitive to near-positivity violations (*i.e.*, when the probability of treatment is close to zero) owing to the first term on the RHS of Eq. (6) [43]. In contrast, the submodel approach will not, because it is constrained due to the regression step.

One of the consequences of finding the efficient IF is that we also achieve improved model robustness. This is because, in cases where multiple plug-in models are used to derive an unbiased estimate, we achieve consistent estimation (*i.e.*, we converge in probability to the true parameter as the sample size increases) even if one of the models is misspecified (*e.g.*, the ATE requires both a propensity score model and an outcome model, and thus the IF facilitates *double* robustness). Furthermore, in cases where both models are well-specified, we achieve efficient estimation. For more technical details on the double robustness property see [28, 39, 65].

Targeted Regularization: Finally, we can use targeted regularization which, to the best of our knowledge, has only been used twice in the NN literature, once in DragonNet [58], and once in TVAE [72], both of which were applied to the task of causal inference. The idea is to solve the efficient influence curve *during* NN training, similarly to Eq. (7), on a per-batch basis. The parameter $\hat{\gamma}$ in Eq. (7) is treated as a learnable parameter, trained as part of the optimization of the NN. The submodel update in Eq. (7) is thereby recast as a regularizer which influences the weights and biases of the outcome model $m(t, \tilde{\mathbf{x}})$. In total, then, the training objective is given by Eq. (8), where \mathcal{L}_i^q is a negative log-likelihood (NLL) of the outcome model $m(t, \tilde{\mathbf{x}})$ which has parameters θ (which comprises NN weights and biases), and \mathcal{L}_i^{tl} is the NLL of the updated outcome model $m(t, \tilde{\mathbf{x}})^*$, which is parameterized by both θ and $\hat{\gamma}$.

$$\mathcal{L} = \min_{\theta} \left[\sum_i^n (\mathcal{L}_i^q + \mathcal{L}_i^{tl}) \right]. \quad (8)$$

As the second NLL term involves the clever covariate H , which in turn involves the plug-in estimator for the propensity score $\pi(Z)$, we will also need a model for the treatment which may be trained via another NLL objective, or integrated into the same NN as the one for the outcome model. Due to the paucity of theoretical analysis for NNs, it is not clear whether targeted regularization provides similar guarantees (debiasing, double-robustness, asymptotic normality) to the one-step and submodel approaches, and this is something we explore empirically.

Conditions for IFs to Work: The conditions necessary for the key relationships above to hold are that our estimator is regular and asymptotically linear such that the sec-

ond order remainder term $o_p(\cdot)$ tends in probability to zero sufficiently quickly. These properties concern the sample size, the smoothness of the estimator, and the quality of the models we are using to approximate the relevant factors of the distribution. Clearly, if our initial model(s) is poor/misspecified then a linear path (or equivalently, a first order VME) will not be sufficient to model the residual distance from the estimand, and the update steps may actually worsen our initial estimate.

In summary, as long as our initial estimator is ‘good enough’ (insofar as it is regular and asymptotically linear), we can describe any residual bias using IFs. Doing so enables us to (a) reduce the residual bias by performing an update to our original estimator using the efficient IF (via the one-step, submodel, or targeted learning approaches), (b) achieve a more robust estimator, and (c) undertake statistical inference (because the updated estimate is normally distributed with a variance equal to the variance of the IF). In order to further demonstrate the relevant concepts, we provide two examples in supplementary, as well as providing the means to analytically derive confidence intervals for purposes of statistical inference.

3.4. Open Questions

The following open questions remain: (1) Can NNs be improved using the one-step, submodel, or targeted regularization approaches? (2) How do NN methods compare against other estimators, with and without IF update techniques? (3) What about estimands for a general graph (*i.e.*, not just the ATE for the graph in Fig. 2)? We aim to answer the first two questions above through an evaluation of different methods (Sec. 6). In particular, we examine the performance of the different approaches in terms of (a) precision in estimation, (b) robustness, and (c) statistical inference. For the third question, we provide the expression of IF for an estimand of a general graph (see supplementary), and also attach the code for doing so automatically.

4. MultiNet

One of the primary considerations when choosing estimation algorithms/models is whether the estimator can represent a family of distributions which is likely to contain the true Data Generating Process (DGP). Indeed, one of the motivations for semiparametrics is to be able to use non-parametric data-driven algorithms which have the flexibility to model complex DGPs, whilst still being able to perform statistical inference.

Early experimentation highlighted to us that even though NNs are flexible universal function approximators [29, 30], they may nonetheless yield estimators which are not ‘good enough’ to enable us to leverage their asymptotic properties (such as bias reduction with IFs). Indeed, the IF update may actually *worsen* the initial estimate, pushing us further

off course (for example, see the probability plots in supplementary comparing CFR and CFR+one-step). This problem arose even for simple datasets with only quadratic features. Consider the Super Learner (SL) [63], which is an ensemble method where a weighted average of predictions from each candidate learner is taken as the output. The advantage of a SL is that the candidate library includes sufficient diversity with respect to functional form and complexity such that the true DGP is likely to fall within the family of statistical models which can be represented by the ensemble. Given that there is nothing preventing the inclusion of multiple NNs of differing complexity and architecture in a SL directly, which can be computationally expensive, we instead attempt to match the diversity and complexity of a SL with a single NN which we call MultiNet.

A block diagram for MultiNet is shown in Figure 1. The method comprises four main elements: a CounterFactual Regression (CFR) network backbone [56], layer-wise optimization, loss masking, and a combination of predictions. CFR is a popular NN method for causal inference tasks. It includes separate outcome arms depending on the treatment condition, and forms the backbone of MultiNet. For each layer in MultiNet, we predict $y|t, \mathbf{x}$ for $t = \{0, 1\}$ and compute the corresponding layerwise cross-entropy loss (for binary outcome). This simulates the multiple outputs of a typical ensemble method - each layer represents a different function of the input.

We explore two variants of this layerwise training. Firstly, we allow each layerwise loss gradient to influence all prior network parameters. This is similar to the implementation of the auxiliary loss idea in the Inception network [60], and we refer to this variant as ‘MN-Inc’. The second variant involves only updating the parameters of the corresponding layer, preventing gradients from updating earlier layers. We call this variant the ‘cascade’ approach, and refer to this variant as ‘MN-Casc’.

In order to increase the diversity across the layers and to approximate the diversity of an ensemble, we explore the use of loss masking. For this, we partition the training data such that each layer has a different ‘view’ of the observations. The loss is masked such that each layer is trained on a different, disjoint subset of the data. We refer to variants of MultiNet with loss masking as ‘MN+LM’. The objective function of MultiNet is therefore:

$$\mathcal{L} = \min \left[\frac{1}{n} \sum_i^n \frac{1}{L} \sum_l^L m_i^l \mathcal{L}_i^l \right] \quad (9)$$

where m_i^l is the mask for datapoint i in layer l (this is set to 1 for variants without loss masking), and \mathcal{L}_i^l is the cross-entropy loss for datapoint i and layer l .

Finally, all variants of MultiNet include a constrained regression over the layerwise predictions. This step is only

applied after MultiNet has been trained. For each treatment condition, we concatenate the layerwise predictions into a matrix \hat{Y} which has shape $(L \times N)$ where L is the number of layers and N is the number of datapoints. We then solve $\hat{Y}^T \beta = y$, with layerwise weights β which are constrained to sum to one and be non-negative. For this we use a SciPy [33] non-negative least squares solver. The weights are then used for subsequent predictions. We may also interpret β to understand which layers are the most useful for solving the constrained regression, but leave this to future work.

5. Experiments

Data: Recent work has highlighted the potential for the performance of modern causal inference methods to be heavily dataset-dependent, and has recommended the use of bespoke datasets which transparently test specific attributes of the evaluated models across different dimensions [11]. We therefore undertake most of the evaluation using a DGP which we refer to as the LF-dataset (v1), which models 1-year mortality risk for cancer patients treated with monotherapy or dual therapy, and which has been used for similar evaluations in the literature [43]. One motivation for starting with this DGP is that its polynomial functional form is not sufficiently complex to unfavourably bias the performance of any method from the start. The dataset also exhibits near-positivity violations, and will therefore highlight problems associated with the propensity score models which are necessary for the update process. We also adjust the level of non-linearity in order to assess the robustness of each method to increased complexity. Accordingly, we introduce an exponential response into the potential outcome under monotherapy ($t = 1$) for the second variant (v2). Our LF-datasets comprise 100 samples from a set of generating equations given in the supplementary. Both variants are designed to highlight problems which may arise due to near positive violations.

The second dataset comprises 100 simulations from the well-known semi-synthetic Infant Health and Development Program (IHDP) dataset [21, 27], each with 747 samples. This dataset represents a staple benchmark for causal inference in machine learning [11]. However, it is worth noting that recent work has shown it to preferentially bias certain estimators [11], so we include this dataset for completeness but discount our interpretation of the results accordingly. Further details are given in the supplementary.

Procedure and Evaluation Criteria: We evaluate a number of different methods in terms of their ability to estimate the ATE. In particular, we compare these methods when combined with IFs via the one-step update, the submodel update, targeted regularization, or combinations thereof. As described above, we are interested in three properties relating to performance: estimation precision, robust-

ness, and normality. Estimation precision is evaluated using mean squared error (MSE) and the standard error (s.e.) of the estimates. Robustness will be evaluated by comparing initial estimators that fail to exhibit the desired properties, with the results once these estimators have been updated via the one-step or submodel approaches. For normality, we examine the empirical distribution of the estimates. Using these distributions, we provide probability plots and p -values from Shapiro-Wilks tests for normality [57]. Doing so provides an indication of the estimator’s asymptotic linearity and whether the IFs are facilitating statistical inference as intended.

Algorithms: We compare linear/logistic regression (LR); a Super Learner (SL) comprising a LR, a LR with extra quadratic features, a Support Vector classifier, a random forest classifier [7], a nearest neighbours classifier [3], and an AdaBoost classifier [20]; an implementation of CFR-net [56] (CFR); and our MultiNet variants (*MN-Inc*, *MN-Casc*, *MN-Inc+LM*, *MN-Casc+LM*). When estimating the IF of the ATE, we also need estimators for the propensity score / treatment model. All methods except CFR-net and MultiNet can be directly adapted for this task. For CFR-net and MultiNet, we simply remove one of the outcome arms, such that we predict $t|x$.

For the NN based methods (CFR and MN), we compare the base networks with the use of the semiparametric modifications including: one-step update, submodel update, targeted regularization (treg), and targeted regularization in combination with the one-step and submodel updates (some combinations are reported in supplementary for brevity). For the semiparametric variants, we explore the use of both equivalent NN based propensity score models (e.g., we combine the CFR outcome model, with an adaptation of CFR for propensity score modeling to be ‘plugged into’ the update expressions), as well as SL based propensity score models.

All non-NN based approaches are implemented using the default algorithms in the scikit-learn package [48]. For all NN methods, we undertake a Monte-Carlo train-test split hyperparameter search with 15 trials, for every one of the 100 samples from the DGP. For fairness, all NN methods have a hyperparameter search across the same search space. For details on hyperparameters see supplementary. The best performing set of hyperparameters is then used to train the network on the full dataset. Note that, unlike in traditional supervised learning tasks, using the full data with causal inference is possible because the target estimand is not the same quantity as the quantity used to fit the algorithms [17]. Indeed, whilst cross-fitting is used for the hyperparameter search, subsequent use of the full data has been shown to be beneficial, especially in small samples [12]. It is reassuring to note that overfitting is likely to worsen our estimates, rather than misleadingly improve them. Similarly,

even though the SL is trained and the corresponding weights derived using a hold-out set, the final algorithm is fit on the full dataset for estimation. Logistic regression is simply fit on the full dataset without any data splitting. For all treatment models, we bound predictions to fall in the range $[-.025, .975]$ [41].

6. Results

We share key results in Table 1. See supplementary for more extensive results (incl. probability plots).

For **LF (v1)**, we see that the base CFR performs significantly worse in all considered metrics than LR and SL. Indeed, base LR and base SL achieve the best results in terms of MSE and s.e., although note that none of the base algorithms achieve asymptotic normality. Notice that LR's base MSE performance on LF (v1) is actually better than its MSE performance using the one-step and submodel updates. Such behaviour has been noted before [43], and occurs when the base learner is already close and/or when both outcome and treatment models are misspecified. Unlike CFR, our *MN-Inc* and *MN-Casc* variants worked well as either outcome or treatment models, yielding the best results with the one-step update. The other two of our *MN*-variants also performed well with the one-step and submodel updates but required a SL treatment model to do so.

The potential improvements for LR in combination with update steps is more striking for **LF (v2)**. Here, the LR base outcome model is quite misspecified (LF v2 has an exponential outcome model). By combining the LR with the SL one-step and submodel update processes enabled the LR method to perform well in spite of the non-linearity of the outcome. This is a demonstration of double-robustness - even though the outcome model is misspecified, the treatment model is not (owing to the use of a SL), and the estimates are improved. As with dataset LF (v1), combining CFR with IFs resulted in a substantial improvement, especially when using an SL treatment model, yielding a competitive MSE, s.e., and normally distributed estimates (thus amenable to statistical inference). These results well demonstrate the power of semiparametric methods for improving our estimation with NNs, and again illustrate the double-robustness property: the CFR outcome model was poorly specified, but was able to recover with an SL treatment model. Similar performance for our *MN*-variants on LF (v1) was observed for (v2).

Unfortunately, no method variant yielded normally distributed estimates with the **IHDP** dataset. The worst performing estimator across any combination of semiparametric techniques was LR. This makes sense given the non-linearity in the IHDP outcome process (see supplementary and [11]). The SL with the one-step or submodel updates performed equally (poorly) as the best CFR and *MN-Casc* variants, although the SL provided smaller s.e.. Overall, the

best methods were our *MN-Inc* and *MN-Inc+LM* variants in combination with either a one-step update, or a one-step update using a SL treatment model.

The MultiNet variant which performed the best and most consistently across **all datasets** was our *MN-Inc* (or equally, *MN-Inc+LM*) with the one-step update. Whereas other methods benefited from the help of a SL treatment model, *MN-Inc* worked well as both an outcome and a treatment model, making it the best all-rounder across datasets, as well as the least dependent on the SL for correction. For all NN based approaches, targeted regularization made little difference, and sometimes resulted in instability and high MSEs. Further work is required to investigate this, although it may relate to which treatment model is used, and associated sensitivity to positivity violations. In the supplementary we provide additional results for combining targeted regularization with a SL treatment model to improve stability, but the results were inconclusive. A prior application also described the potential for the regularization to be inconsistent [58].

Finally, for all base learners, we observe the potential for improvement using the semiparametric techniques, primarily for improving the associated MSE. It is also worth noting that in general, the base CFR method has consistently higher s.e. than the *MN*-variants, although combining CFR with an update step (*e.g.*, one-step w/ SL) significantly reduced the s.e..

7. Discussion, Limitations, and Conclusion

In this paper we have introduced some key aspects of semiparametric theory, undertaken an evaluation of the potential of semiparametric techniques to provide a 'free' performance improvement for existing estimators without needing more data, and without needing to retrain them. We also proposed a new pseudo-ensemble NN method 'MultiNet' for simulating an ensemble approach with a single network, and provided the expression and code for deriving influence functions for estimands from a general graph automatically. The results demonstrated that semiparametric techniques can be used to improve existing estimators in terms of estimation error, normality, and standard error, whether they be linear regressors, or NNs. Our MultiNet provided the most consistent improvements across datasets. Some interesting additional findings highlighted difficulties with training NNs for estimation tasks. It is important to remember that, in practice, we will not have access to the true ATE, and practitioners should exercise caution when using NNs because it will be difficult to assess their performance without ground-truth. Furthermore, and in terms of societal impact, it is important to remember that the reliability of causal estimates depend on strong, untestable assumptions.

Despite this work providing evidence for the relevance

Table 1. Mean squared errors (MSE) and standard error (s.e.) (lower is better) and Shapiro-Wilks test p -values for normality (higher is better) for 100 simulations. Best results are those competing across all three dimensions. **Bold** indicates best result for each algorithm, **bold and underline** indicates best result for each dataset variant. Multiple methods may perform equally well.

Dataset	Algorithm	Base			One-Step			Submod			Treg			Treg+Submod			One-Step w/ SL			Submod w/ SL		
		p	MSE	s.e.	p	MSE	s.e.	p	MSE	s.e.	p	MSE	s.e.	p	MSE	s.e.	p	MSE	s.e.	p	MSE	s.e.
LF (v1)	LR	.001	.0004	.002	.276	.0007	.003	.248	.0008	.003	-	-	-	-	-	-	.378	.0006	.003	.591	.0008	.003
	SL	.001	.0004	.002	.53	.0008	.003	.651	.0009	.003	-	-	-	-	-	-	-	-	-	-	-	-
	CFR	.0	.0114	.008	.001	.0042	.004	.01	.01	.003	.07	.0113	.008	.0	.0105	.002	.396	.0006	.003	.909	.0015	.003
	MN-Inc	.052	.0008	.003	.78	.0007	.003	.394	.001	.003	.729	.0012	.003	.681	.001	.003	.639	.0008	.003	.329	.001	.003
	MN-Inc+LM	.135	.0009	.003	.141	.0007	.003	.578	.0009	.003	.0	.0017	.004	.957	.0011	.003	.969	.0008	.003	.786	.0009	.003
	MN-Casc	.0	.0018	.004	.231	.0014	.002	.0	.0018	.003	.083	.0086	.007	.702	.0045	.004	.831	.0007	.003	.339	.0009	.003
	MN-Casc+LM	.053	.0058	.006	.018	.002	.003	.204	.0037	.003	.0	.0091	.008	.74	.0036	.003	.747	.0007	.003	.625	.001	.003
LF (v2)	LR	.066	.0024	.002	.752	.0007	.003	.497	.0008	.003	-	-	-	-	-	-	.785	.0007	.003	.867	.0009	.003
	SL	.349	.0017	.003	.938	.0008	.003	.92	.0009	.003	-	-	-	-	-	-	-	-	-	-	-	-
	CFR	.0	.0185	.01	.0	.006	.005	.0	.0151	.002	.0	.035	.01	.008	.0162	.002	.623	.0007	.003	.065	.0015	.003
	MN-Inc	.119	.001	.003	.204	.0006	.003	.211	.0008	.003	.002	.0009	.002	.029	.0008	.003	.058	.0007	.003	.049	.0008	.003
	MN-Inc+LM	.0	.0011	.003	.438	.0009	.003	.813	.0011	.003	.139	.0071	.005	.678	.0026	.003	.959	.0005	.002	.949	.0009	.003
	MN-Casc	.0	.002	.004	.013	.0033	.002	.892	.0043	.003	.77	.014	.006	.365	.0101	.002	.272	.0007	.003	.264	.0011	.003
	MN-Casc+LM	.257	.0113	.007	.349	.0032	.003	.001	.0083	.002	.066	.0295	.007	.0	.0112	.002	.897	.0006	.003	.241	.0013	.003
IHDP	LR	.022	.1818	.019	.0	.0576	.035	.0	.0461	.044	-	-	-	-	-	.0	.1322	.019	.0	.0597	.03	
	SL	.0	.0466	.032	.0	.0311	.033	.0	.0346	.034	-	-	-	-	-	-	-	-	-	-	-	
	CFR	.0	.7709	.098	.0	.2865	.074	.0	.0439	.052	.0	25.5	.3	.0	.0604	.051	.0	.2626	.063	.0	1.7	.114
	MN-Inc	.0	.0324	.042	.0	.0297	.044	.0	8.7	.299	.0	.0482	.042	.0	30.8	.537	.0	.0243	.044	.0	.0425	.042
	MN-Inc+LM	.0	.0393	.045	.0	.0259	.043	.0	.9849	.099	.0	.1332	.038	.0	1.9	.138	.0	.0243	.044	.0	.0327	.042
	MN-Casc	.0	.1977	.046	.0	.0737	.04	.0	.064	.04	.0	2.9	.115	.0	.102	.042	.0	.0816	.042	.0	.0383	.047
	MN-Casc+LM	.0	4.7	.158	.0	1.4	.093	.0	.2118	.049	.0	23.9	.164	.0	.1824	.06	.0	1.1	.079	.0	4.7	.202

of semiparametric theory for machine learning, many open questions remain: a similar set of experiments should be undertaken for other estimands (such as the conditional ATE); the sensitivity of the different methods to sample size should be evaluated. Also, one may derive higher order IFs [8, 54, 67, 68] which introduce new challenges and opportunities.

References

- [1] A.M. Alaa and M. van der Schaar. Validating causal inference models via influence functions. *ICLR*, 2019. 3
- [2] A.M. Alaa and M. van der Schaar. Discriminative jackknife: Quantifying uncertainty in deep learning via higher-order influence functions. *arXiv preprint*, arXiv:2007.13481v1, 2020. 3
- [3] N. S. Altman. An introduction to kernel and nearest-neighbor nonparametric regression. *The American Statistician*, 46(3):175–185, 1992. 7
- [4] I. Bica, A.M. Alaa, C. Lambert, and M. van der Schaar. From real-world patient data to individualized treatment effects using machine learning: Current and future methods to address underlying challenges. *Clinical Pharmacology and Therapeutics*, 109(1):87–100, 2020. 2
- [5] P.J. Bickel, C.A.J. Klassen, Y. Ritov, and J.A. Wellner. *Efficient and Adaptive Estimation for Semiparametric Models*. Springer-Verlag, New York, 2007. 2
- [6] M.J. Blanca, R. Alarcon, and R. Bono. Current practices in data analysis procedures in psychology: what has changed? *Frontiers in Psychology*, 2018. 1
- [7] L. Breiman. Random forests. *Machine Learning*, 45(1):5–32, 2001. 7
- [8] M. Carone, I. Diaz, and M.J. van der Laan. Higher-order targeted minimum loss-based estimation. *U.C. Berkeley Division of Biostatistics Working Paper Series*, 2014. 9
- [9] V. Chernozhukov, D. Chetverikov, M. Demirer, E. Duflo, C. Hansen, W. Newey, and J. Robins. Double/debiased machine learning for treatment and structural parameters. *Econometrics Journal*, 21:C1–C68, 2018. 3
- [10] A. Curth, A.M. Alaa, and M. van der Schaar. Estimating structural target functions using machine learning and influence functions. *arXiv preprint*, arXiv:2008.06461v3, 2021. 2, 3
- [11] A. Curth, D. Svensson, J. Weatherall, and M. van der Schaar. Really doing great at estimating CATE? a critical look at ML benchmarking practices in treatment effect estimation. *35th Conference on Neural Information Processing Systems (NeurIPS 2021)*, 2021. 2, 3, 7, 8, 17, 18
- [12] A. Curth and M. van der Schaar. Nonparametric estimation of heterogeneous treatment effects: From theory to learning algorithms. *AISTATS*, 130, 2021. 2, 3, 7
- [13] V. Dorie. Non-parametrics for causal inference. <https://github.com/vdorie/npci>, 2016. 17
- [14] S.C. Endres, S.C. Sandrock, and C. Focke. A simplicial homology algorithm for Lipschitz optimization. *Journal of Global Optimization*, 72:181–217, 2018. 18
- [15] R.J. Evans and T.S. Richardson. Smooth, identifiable supermodels of discrete DAG models with latent variables. *Bernoulli*, 25(2):848–876, 2019. 15
- [16] M. Ezzati, A.D. Lopez, and C.J.L. Murray, editors. *Comparative Quantification of Health Risks: Global and Regional Burden of Disease Attributable to Selected Major Risk Factors*, chapter Effects of multiple interventions. World Health Organization, Geneva, 2004. 15
- [17] M.H. Farrell, T. Liang, and S. Misra. Deep neural networks for estimation and inference. *arXiv preprint*, arXiv:1809.09953v3, 2019. 7
- [18] A. Fisher and E.H. Kennedy. Visually communicating and teaching intuition for influence functions. *arXiv:1810.03260v3*, 2019. 4

- [19] M. Fréchet. Sur les ensembles de fonctions et les operations lineaires. *Les Comptes rendus de l'Académie des sciences*, 144, 1907. 4, 13
- [20] Y. Freund and R. Schapire. A decision-theoretic generalization of on-line learning and application to boosting. *Journal of Computer and System Sciences*, 55(1):119–139, 1997. 7
- [21] R. T. Gross. *Infant health and development program (IHDP): enhancing the outcomes of low birth weight, premature infants in the United States*. MI: Inter-university Confortium for Political and Social Research, Ann Arbor, 1993. 7
- [22] C. Guo, G. Pleiss, Y. Sun, and K.Q. Weinberger. On calibration of modern neural networks. *ICLR*, 2017. 19
- [23] R. Guo, L. Cheng, J. Li, P.R. Hahn, and H. Liu. A survey of learning causality with data: Problems and methods. *ACM Comput. Surv.*, 1(1), 2020. 3
- [24] R. Guo, J. Li, and H. Liu. Learning individual causal effects from networked observational data. *Association for Computing Machinery*, 2020. 12
- [25] F. R. Hampel. The influence curve and its role in robust estimation. *Journal of the American Statistical Association*, 69(346):383–393, 1974. 4
- [26] X. Han, B.C. Wallace, and Y. Tsvetkov. Explaining black box predictions and unveiling data artifacts through influence functions. *arXiv preprint*, arXiv:2005.06675v1, 2020. 2, 3
- [27] J. L. Hill. Bayesian nonparametric modeling for causal inference. *Journal of Computational and Graphical Statistics*, 20(1), 2011. 7, 17
- [28] O. Hines, O. Dukes, K. Diaz-Oraz, and S. Vansteelandt. Demystifying statistical learning based on efficient influence functions. *arXiv preprint*, arXiv:2107.00681, 2021. 4, 5, 13, 14
- [29] K. Hornik. Some new results on neural network approximation. *Neural Networks*, 6:1069–1072, 1993. 6
- [30] K. Hornik, M. Stinchcombe, and H. White. Multilayer feed-forward networks are universal approximators. *Neural Networks*, 2:359–366, 1989. 6
- [31] Y. Huang and M. Valtorta. Pearl’s calculus of intervention is complete. *arXiv preprint*, arXiv:1206.6831, 2012. 15
- [32] G.W. Imbens and D.B. Rubin. *Causal inference for statistics, social, and biomedical sciences. An Introduction*. Cambridge University Press, New York, 2015. 3, 12
- [33] E. Jones, T. Oliphant, P. Petereson, and et al. SciPy: Open source scientific tools for Python. <http://www.scipy.org>, 2001. 7, 18
- [34] K. Kandasamy, A. Krishnamurthy, B. Poczos, L. Wasserman, and J.M. Robins. Influence functions for machine learning: nonparametric estimators for entropies, divergences and mutual informations. *arXiv:1411.4342v3*, 2015. 13
- [35] E.H. Kennedy. Semiparametric theory and empirical processes in causal inference. *arXiv:1510.04740v3*, 2016. 4
- [36] E.H. Kennedy. Optimal doubly robust estimation of heterogeneous causal effects. *arXiv preprint*, arXiv:2004.14497v2, 2020. 3
- [37] P.W. Koh and P. Liang. Understanding black-box predictions via influence curves. *PMLR*, 2017. 2, 3
- [38] N. Kreif and K. DiazOrdaz. Machine learning in policy evaluation: new tools for causal inference. *arXiv:1903.00402v1*, 2019. 3
- [39] C.F. Kurz. Augmented inverse probability weighting and the double robustness property. *Medical Decision Making*, 2021. 5
- [40] J. Levy. Tutorial: Deriving the efficient influence curve for large models. *arXiv:1903.01706v3*, 2019. 4
- [41] H. Li, S. Rosete, J. Coyle, R.V. Phillips, N.S. Hejazi, I. Malenica, B.F. Arnold, J. Benjamin-Chung, A. Mertens, J.M. Colford, M.J. van der Laan, and A.E. Hubbard. Evaluating the robustness of targeted maximum likelihood estimators via realistic simulations in nutrition intervention trials. *arXiv preprint*, arXiv:2109.14048v1, 2021. 3, 8
- [42] C. Louizos, U. Shalit, J. Mooij, D. Sontag, R. Zemel, and M. Welling. Causal effect inference with deep latent-variable models. *31st Conference on Neural Information Processing Systems*, 2017. 2, 3
- [43] M.A. Luque-Fernandez, M. Schomaker, B. Rachet, and M.E. Schnitzer. Targeted maximum likelihood estimation for a binary treatment: A tutorial. *Statistics in Medicine*, 37(16):2530–2546, 2018. 3, 5, 7, 8, 17
- [44] R. Neugebauer and M.J. van der Laan. Why prefer double robust estimates? illustration with causal point treatment studies. *Journal of Statistical Planning and Inference*, 129(1):405–426, 2005. 5
- [45] J. Pearl. *Causality*. Cambridge University Press, Cambridge, 2009. 3
- [46] J. Pearl. On a class of bias-amplifying variables that endanger effect estimates. *arXiv:1203.3503*, 2012. 3
- [47] J. Pearl, M. Glymour, and N.P. Jewell. *Causal inference in statistics: A primer*. Wiley, 2016. 3
- [48] F. Pedregosa, G. Varoquaux, A. Gramfort, V. Michel, and B. et al. Thirion. Scikit-learn: Machine learning in Python. *JMLR*, 12:2825–2830, 2011. 7
- [49] M. Petersen, L. Balzer, D. Kwarsiima, N. Sang, G. Chamie, J. Ayieko, J. Kabami, A. Owaraganise, T. Liegler, F. Mwangwa, and K. Kadede. Association of implementation of a universal testing and treatment intervention with HIV diagnosis, receipt of antiretroviral therapy, and viral suppression in East Africa. *Journal of American Medical Association*, 317(21):2196–2206, 2017. 3
- [50] T.S. Richardson, R.J. Evans, J.M. Robins, and I. Shpitser. Nested Markov properties for Acyclic Directed Mixed Graphs. *arXiv preprint*, arXiv:1701.06686v2, 2017. 15
- [51] T.S. Richardson and P. Spirtes. Causal inference via ancestral graph models. In P. Green, N. Hjort, and S. Richardson, editors, *Highly Structured Stochastic Systems*. Oxford University Press, Oxford, 2003. 15
- [52] F. Riesz. Sur les operations fonctionnelles lineaires. *Comptes rendus de l'Académie des Sciences*, 149, 1909. 4, 13
- [53] J. Robins. A new approach to causal inference in mortality studies with a sustained exposure period - application to control of the healthy worker survivor effect. *Mathematical Modelling*, 7:1393–1512, 1986. 15
- [54] J.M. Robins, L. Li, E.J. Tchetgen, and A.W. van der Vaart. Higher order influence functions and minimax estimation of

- nonlinear functionals. *Probability and Statistics: Essays in Honor of David A. Freedman*, pages 335–421, 2008. [9](#)
- [55] D. B. Rubin. Causal inference using potential outcomes: Design, modeling, decisions. *Journal of the American Statistical Association*, 100(469):322–331, 2005. [12](#)
- [56] U. Shalit, F. D. Johansson, and D. Sontag. Estimating individual treatment effect: generalization bounds and algorithms. *arxiv:1606.03976v5*, 2017. [2, 3, 6, 7, 17](#)
- [57] S.S. Shapiro and M.B. Wilk. An analysis of variance test for normality (complete samples). *Biometrika*, 52(3-4):591–611, 1965. [7](#)
- [58] C. Shi, D. M. Blei, and V. Veitch. Adapting neural networks for the estimation of treatment effects. *33rd Conference on Neural Information Processing Systems*, 2019. [3, 5, 8, 17](#)
- [59] B. Siegerink, W. den Hollander, M. Zeegers, and R. Middelburg. Causal inference in law: an epidemiological perspective. *European Journal of Risk Regulation*, 7(1):175–186, 2016. [3](#)
- [60] C. Szegedy, W. Liu, Y. Jia, P. Sermanet, S. Reed, D. Anguelov, D. Erhan, V. Vanhoucke, and A. Rabinovich. Going deeper with convolutions. *CVPR*, 2015. [6](#)
- [61] J. Tian and J. Pearl. A general identification condition for causal effects. *AAAI*, 2002. [15](#)
- [62] A. Tsiatis. *Semiparametric Theory and Missing Data*. Springer, New York, 2006. [2, 4, 13](#)
- [63] M.J. van der Laan, E.C. Polley, and A.E. Hubbard. Super Learner. *Statistical Applications of Genetics and Molecular Biology*, 6(25), 2007. [2, 6](#)
- [64] M. J. van der Laan and S. Gruber. Targeted minimum loss based estimation of causal effects of multiple time point interventions. *Int. J. Biostat*, 8: Art 9(41), 2012. [1](#)
- [65] M. J. van der Laan and S. Rose. *Targeted Learning - Causal Inference for Observational and Experimental Data*. Springer International, New York, 2011. [1, 2, 3, 5, 15](#)
- [66] M. J. van der Laan and R. J. C. M. Starman. Entering the era of data science: targeted learning and the integration of statistics and computational data analysis. *Advances in Statistics*, 2014. [1, 2](#)
- [67] M. J. van der Laan, Z. Wang, and L. van der Laan. Higher order targeted maximum likelihood estimation. *arXiv:2101.06290v3*, 2021. [9](#)
- [68] A.W. van der Vaart. Higher order tangent spaces and influence functions. *Statistical Science*, 29(4):679–686, 2014. [9](#)
- [69] T. Verma and J. Pearl. Equivalence and synthesis of causal models. *Proc. 6th Conf. on Uncertainty in Artificial Intelligence*, 1990. [15](#)
- [70] M.J. Vowels, N.C. Camgoz, and R. Bowden. D’ya like DAGs? A survey on structure learning and causal discovery. *arXiv:2103.02582*, 2021. [3](#)
- [71] M. J. Vowels. Misspecification and unreliable interpretations in psychology and social science. *Psychological Methods*, 2021. [1, 4](#)
- [72] M. J. Vowels, N.C. Camgoz, and R. Bowden. Targeted VAE: Structured inference and targeted learning for causal parameter estimation. *IEEE SMDS*, 2021. [3, 5, 12](#)
- [73] D.H. Wolpert and W.G. Macready. No free lunch theorems for optimization. *IEEE Transactions on Evolutionary Computation*, 1(67), 1997. [2](#)
- [74] P.A. Wu and K. Fukumizu. Causal mosaic: cause-effect inference via nonlinear ICA and ensemble method. *AISTATS*, 108, 2020. [2](#)
- [75] P.A. Wu and K. Fukumizu. Intact-VAE: Estimating treatment effects under unobserved confounding. *arXiv:2101.06662v2*, 2021. [3](#)
- [76] L. Yao, Z. Chu, S. Li, Y. Li, J. Gao, and A. Zhang. A survey on causal inference. *arXiv:2002.02770*, 2020. [12](#)
- [77] L. Yao, S. Li, Y. Li, M. Huai, J. Gao, and A. Zhang. Representation learning for treatment effect estimation from observational data. *32nd Conference on Neural Information Processing Systems (NeurIPS)*, 2018. [17](#)
- [78] J. Yoon, J. Jordan, and M. van der Schaar. GANITE: Estimation of individualized treatment effects using generative adversarial nets. *ICLR*, 2018. [2, 3](#)

Supplementary Material

Overview of Supplementary Material: This Supplementary Material accompanies the work ‘A Free Lunch with Influence Functions? Improving Neural Network Estimates with Concepts from Semiparametric Statistics’. As per the provided table of contents, we provide an overview of key concepts in causal inference, including the most common causal assumptions (positivity, ignorability, and the stable unit value assumptions) in Sections A and B. We then provide an introduction to influence functions (IFs) with some demonstrative examples, as well as providing the means to derive confidence intervals from IFs in Section C. Then, we provide the expression for the influence function of a general estimand for a given graph (note also the associated code) in Section D.⁵ We then provide details about the data used in the experiments and the hyperparameter searches undertaken for the neural network methods in Sections E and F. We provide additional experimental results (including probability plots) and discussion in Section G, and finally we note some ideas we implemented but which did not work in Section H.

A. Overview of Causal Inference

Fig. 2(a) is characteristic of observational data, where the outcome is related to the covariates as well as the treatment, and treatment is also related to the covariates. For example, if we consider age to be a typical covariate, young people may opt for surgery, whereas older people may opt for medication. Assuming that an age-related risk mechanism exists, then age will confound our estimation of the causal effect of treatment on outcome. One of the goals of a Randomized Controlled Trial (RCT) is to reduce this confounding by making the assignment of treatment (asymptotically) statistically independent of treatment by randomly assigning it. This enables us to compare the outcomes for the people who were treated, and those who were not (or equivalently to compare multiple alternative treatments).

One of the most common causal estimands is the Average Treatment Effect (ATE): $\tau(\mathbf{x}) = \mathbb{E}_{\mathbf{x}}[\mathbb{E}[y(1)|\mathbf{x}] - \mathbb{E}[y(0)|\mathbf{x}]]$. Here, $y(1)$ and $y(0)$ are what are known as *potential outcomes* for the outcome under treatment and the outcome under no treatment, respectively [32]. In practice, we only have access to one of these two quantities, whilst the other is missing, and as such the typical supervised learning paradigm does not apply. One approach to the problem is using Pearl’s *do*-calculus, which enables us to re-frame the ATE in terms of the *do* operator: $\tau(X) = \mathbb{E}_{\mathbf{x}}[\mathbb{E}[y|\mathbf{x}, \text{do}(t = 1)] - \mathbb{E}[y|\mathbf{x}, \text{do}(t = 0)]]$. The *do* operator simulates an intervention, setting treatment to a partic-

ular value regardless of what was observed. In Fig. 2(b), such an intervention removes the dependence of t on \mathbf{x} , and this graph is the same as the one for an RCT, where the treatment is unrelated to the covariates (notwithstanding finite sample correlations). Using *do*-calculus we can establish whether, under a number of strong assumptions⁶, the desired causal estimand can be expressed in terms of the observed joint distribution, and thus whether the effect is *identifiable*. Causal identification and the associated assumptions are both extremely important topics in their own right, but fall beyond the scope of this paper (we are primarily concerned with estimation). Suffice it to say that for the graph in Fig. 2(a), the outcome under intervention can be expressed as:

$$P(y|\text{do}(t = t^*)) = \int_{\mathbf{x}} P(y|\mathbf{x}, t^*)P(\mathbf{x}), \quad (10)$$

which is estimable from observational data. Here, t^* is the specific intervention of interest (*e.g.*, $t^* = 1$). In particular, it tells us that adjusting for the covariates \mathbf{x} is sufficient to remove the bias induced through the ‘backdoor’ path $\mathbf{x} \rightarrow t \rightarrow y$. This particular approach is sometimes referred to as backdoor adjustment. Once we have the expression in Eq. (10), we can shift our focus towards its estimation. Note that even once the problem has been recast as an estimation problem, it differs from the typical problem encountered in supervised learning. Indeed, instead of simply learning a function, we wish to indirectly learn the *difference* between two functions, where these functions represent ‘response surfaces’ - *i.e.*, the outcome/response under a particular treatment.

One may use a regression to approximate the integral in Eq. (10), and indeed, plug-in estimators \hat{Q} can be used for estimating the ATE as:

$$\hat{\tau}(\hat{Q}; \mathbf{x}) = \frac{1}{n} \sum_{i=1}^n (\hat{Q}(1, \mathbf{x}_i) - \hat{Q}(0, \mathbf{x}_i)), \quad (11)$$

B. Causal Assumptions

The causal quantity can be estimated in terms of observational (and therefore statistical) quantities if a number of strong (but common [24, 32, 55, 72, 76]) assumptions hold: (1) Stable Unit Treatment Value Assumption (SUTVA): the potential outcomes for each individual or data unit are independent of the treatments assigned to all other individuals. (2) Positivity: the assignment of treatment probabilities are non-zero and non-deterministic $p(t = t_i|\mathbf{x} = \mathbf{x}_i) > 0, \forall t, \mathbf{x}$. (3) Ignorability/Unconfoundedness/Conditional Exchangeability: There are no unobserved confounders,

⁵Code for models, experiments, and automatic IF derivation is accessible here: https://github.com/matthewvowels1/semiparametrics_and_NNs_release/.

⁶These assumptions are the Stable Unit Treatment Value Assumption (SUTVA), Positivity, and Ignorability/Unconfoundedness - see Section B below for more information.

such that the likelihoods of treatment for two individuals with the same covariates are equal, and the potential outcomes for two individuals with the same latent covariates are also equal s.t. $t \perp\!\!\!\perp (y(1), y(0)) | \mathbf{x}$.

C. Introduction to IFs

This section has been adapted from [28, 34, 62].

Consider the task of estimating a parameter or quantity of a true distribution $\Psi(\mathcal{P})$, where Ψ is the function mapping our distribution to the target quantity, and \mathcal{P} is the true data generating distribution. As an example, consider the targeted estimand to be the expectation $\mathbb{E}[Y]$, where Y is a random variable constituting \mathcal{P} . This can be expressed as:

$$\mathbb{E}[Y] = \Psi(\mathcal{P}) = \int y d\mathcal{P}(y). \quad (12)$$

In practice, rather than \mathcal{P} we may instead only have access to $\hat{\mathcal{P}}_n$, which may be arbitrary. For instance, it could constitute a histogram estimate for a density function. Alternatively, and continuing our example, $\hat{\mathcal{P}}_n$ could be the empirical/sample distribution, in which case our expectation example may be approximated as follows:

$$\Psi(\hat{\mathcal{P}}_n) \approx \Psi(\mathcal{P}) = \frac{1}{n} \sum_{i=1}^n y_i, \quad (13)$$

where the subscript n is the sample size. The degree to which our resulting estimator is biased can be expressed as the difference:

$$\sqrt{n}(\Psi(\hat{\mathcal{P}}_n) - \Psi(\mathcal{P})). \quad (14)$$

Here, the \sqrt{n} scales the difference such that when the difference converges in distribution, then we can also say that the difference converges at a parametric root- n rate. For the expectation of Y we have:

$$\begin{aligned} \sqrt{n}(\Psi(\hat{\mathcal{P}}_n) - \Psi(\mathcal{P})) &= \sqrt{n} \left(\int y d\hat{\mathcal{P}}_n(y) - \int y d\mathcal{P}(y) \right) \\ &= \frac{1}{\sqrt{n}} \sum_i^n (Y_i - \mu) \xrightarrow{\mathcal{D}} \mathcal{N}(0, \sigma^2), \end{aligned} \quad (15)$$

where μ and σ^2 are the mean and variance of Y , respectively, and the second line is a consequence of the central limit theorem. This shows that the empirical approximation of the estimand is an unbiased estimator (the difference converges in probability to zero). However, in many cases $\hat{\mathcal{P}}_n$ is not equivalent to the sample distribution, perhaps because some or all of $\hat{\mathcal{P}}_n$ is being modelled with estimators. As a result, the error does not converge in probability to

zero and some residual error remains. This situation can be expressed as follows [62]:

$$\sqrt{n}(\Psi(\hat{\mathcal{P}}_n) - \Psi(\mathcal{P})) = \frac{1}{\sqrt{n}} \sum_{i=1}^n \phi(y_i, \mathcal{P}) + o_p(1). \quad (16)$$

Here, ϕ is being used to model the residual bias that stems from the fact that $\hat{\mathcal{P}}_n$ is no longer equivalent to a direct sample from \mathcal{P} , and we will discuss the details relating to this function shortly. The $o_p(1)$ term denotes an order 1 convergence in probability to zero which, if we scale the difference by \sqrt{n} , thereby yielding our $1/\sqrt{n}$ parametric convergence rate.

If we assume that the difference is asymptotically linear, then we can represent $\hat{\mathcal{P}}_n$ as a perturbed version of \mathcal{P} . This also results in convergence in distribution as follows:

$$\begin{aligned} \frac{1}{\sqrt{n}} \sum_i^N \phi(Z_i, \mathcal{P}) &\xrightarrow{\mathcal{D}} \mathcal{N}(0, \mathbb{E}(\phi\phi^T)), \\ \sqrt{n}(\Psi(\hat{\mathcal{P}}_n) - \Psi(\mathcal{P})) &\xrightarrow{\mathcal{D}} \mathcal{N}(0, \mathbb{E}(\phi\phi^T)). \end{aligned} \quad (17)$$

We can imagine the sample distribution lies on a linear path towards the true distribution \mathcal{P} . This linear model can be expressed using what is known as parametric submodel, which represents a family of distributions indexed by a parameter ϵ :

$$\mathcal{P}_\epsilon = \epsilon \hat{\mathcal{P}}_n + (1 - \epsilon) \mathcal{P}. \quad (18)$$

It can be seen that when $\epsilon = 0$, we arrive at the true distribution, and when $\epsilon = 1$, we are at our current empirical distribution or model of the true distribution. We can therefore use this submodel to represent the perturbation from where we want to be \mathcal{P} in the direction of where we are with our current estimator(s) $\hat{\mathcal{P}}_n$. The direction associated with \mathcal{P}_ϵ can then be expressed as a pathwise derivative in terms of the function representing our estimand Ψ :

$$\frac{d\Psi(\epsilon \hat{\mathcal{P}}_n + (1 - \epsilon) \mathcal{P})}{d\epsilon}. \quad (19)$$

When this derivative exists (under certain regularity conditions), it is known as the Gateaux derivative. We can evaluate this when $\epsilon = 0$ (*i.e.*, evaluated at the true distribution according to the parametric submodel). Then by the Riesz representation theorem [19, 52], we can express the linear functional in Eq. (19) evaluated at $\epsilon = 0$ as an inner product between a functional ϕ and its argument:

$$\begin{aligned} &\left. \frac{d\Psi(\epsilon \hat{\mathcal{P}}_n + (1 - \epsilon) \mathcal{P})}{d\epsilon} \right|_{\epsilon=0} \\ &= \int \phi(y, \mathcal{P}) \{d\hat{\mathcal{P}}_n(y) - d\mathcal{P}(y)\}. \end{aligned} \quad (20)$$

The function ϕ is the *Influence Function* (IF) evaluated at the distribution \mathcal{P} in the direction of y . Eq. (20) can be substituted back into Eq. (16) to yield:

$$\begin{aligned} & \sqrt{n}(\Psi(\hat{\mathcal{P}}_n(y)) - \Psi(\mathcal{P}(y))) \\ &= \int \phi(y, \mathcal{P}) \{d\hat{\mathcal{P}}_n(y) - d\mathcal{P}(y)\} + o_p(1), \end{aligned} \quad (21)$$

which equivalently allows us to express the estimate of the target quantity as:

$$\begin{aligned} \Psi(\hat{\mathcal{P}}_n) &= \\ \Psi(\mathcal{P}) + \left. \frac{d\Psi(\epsilon\hat{\mathcal{P}}_n + (1-\epsilon)\mathcal{P})}{d\epsilon} \right|_{\epsilon=0} &+ o_p(1/\sqrt{n}). \end{aligned} \quad (22)$$

Eq. (22) expresses the estimated quantity $\Psi(\hat{\mathcal{P}}_n)$ in terms of the true quantity $\Psi(\mathcal{P})$, whereas it would be more useful to do so the other way around, such that we have the true quantity in terms of things we can estimate. Hines et al. [28] provide an exposition in terms of the Von Mises expansion (the functional analogue of the Taylor expansion) such that the true quantity can be expressed as:

$$\Psi(\mathcal{P}) = \Psi(\hat{\mathcal{P}}_n) + \frac{1}{n} \sum_i^n \phi(y_i, \hat{\mathcal{P}}_n) + o_p(1/\sqrt{n}). \quad (23)$$

Which, it can be seen, is in the same form as Eq. (22), except that ϕ is being evaluated at $\hat{\mathcal{P}}_n$, rather than \mathcal{P} . This also accounts for the change in direction otherwise absorbed by a minus sign when expressing $\Psi(\mathcal{P})$ in terms of $\Psi(\hat{\mathcal{P}}_n)$. Finally, note that in Eq. 20 the pathwise derivative is expressed the expectation of ϕ . However, in cases where we substitute $\hat{\mathcal{P}}$ for a Dirac function (see Sec. C.1 for an example), the integral will evaluate to the value of ϕ at one specific point. Of course, if we have multiple values we wish to evaluate at (e.g. an empirical distribution represented with Dirac delta functions at each point), then the result is the empirical approximation to the expectation, as indicated by the $\frac{1}{n} \sum_i^n$ notation in Eq. 23.

C.1. Demonstration by Example

Population Mean: As before, we start with the expected value of Y , otherwise known as the population mean. As above, the IF for the population mean $\Psi(\mathcal{P}) = \int yf(y)dy$ can be derived by substituting $f_\epsilon(y) = \epsilon\delta_{\tilde{y}}(y) + (1-\epsilon)f(y)$ for $f(y)$, differentiating, and setting $\epsilon = 0$ [28]:

$$\begin{aligned} \Psi(\mathcal{P}_\epsilon) &= \int y(\epsilon\delta_{\tilde{y}}(y) + (1-\epsilon)f(y))dy \\ &= \epsilon\tilde{y} + (1-\epsilon)\Psi(\mathcal{P}), \end{aligned} \quad (24)$$

$$\phi(\tilde{y}, \mathcal{P}) = \tilde{y} - \Psi(\mathcal{P}). \quad (25)$$

Here, $\delta_{\tilde{y}}$ is the Dirac delta function at the point at which $y = \tilde{y}$, where \tilde{y} can be a point in our empirical sample. We substitute the IF in Eq. (25) into Eq. (23). Once again, we express the true estimand as a function of the estimated quantities (rather than the other way around) by evaluating derivative under distribution $\hat{\mathcal{P}}_n$ in directions \tilde{y} from the empirical distribution $\hat{\mathcal{P}}_n$ giving:

$$\Psi(\mathcal{P}) = \Psi(\hat{\mathcal{P}}_n) + \frac{1}{n} \sum_i^n [\tilde{y}_i - \Psi(\hat{\mathcal{P}}_n)] + o_p\left(\frac{1}{\sqrt{n}}\right). \quad (26)$$

But note that $\frac{1}{n} \sum_i^n \Psi(\hat{\mathcal{P}}_n) = \Psi(\hat{\mathcal{P}}_n)$ and $\sum_i^n \tilde{y}_i = \Psi(\hat{\mathcal{P}}_n)$, thereby illustrating again that in the case of the expectation, there is no residual bias to model, and we arrive back at Eq. (15).

Average Treatment Effect (ATE): A second example concerns the ATE, which we can break down in terms of an expected difference between two potential outcomes. For the DAG: $T \rightarrow Y, T \leftarrow X \rightarrow Y$ (also see Fig. 2), the expectation of the potential outcome under treatment can be expressed as [28]:

$$\begin{aligned} \Psi(\mathcal{P}) &= \mathbb{E}_X[\mathbb{E}_Y[Y|T=t, X]] \\ &= \int yf(y|t, \mathbf{x})f(\mathbf{x})dyd\mathbf{x} \\ &= \int \frac{yf(y, t, \mathbf{x})f(\mathbf{x})}{f(t, \mathbf{x})}dyd\mathbf{x}, \end{aligned} \quad (27)$$

where $Z = (X, T, Y)$. Following the same steps as before, the IF can be derived as:

$$\phi(Z, \mathcal{P}_\epsilon) = \int y \left. \frac{d}{d\epsilon} \right|_{\epsilon=0} \frac{yf(y, t, \mathbf{x})f(\mathbf{x})}{f(t, \mathbf{x})} dyd\mathbf{x}. \quad (28)$$

Substituting each density e.g.,

$$f_\epsilon(y, t, \mathbf{x}) = \epsilon\delta_{\tilde{y}, \tilde{t}, \tilde{\mathbf{x}}}(y, t, \mathbf{x}) + (1-\epsilon)f(y, t, \mathbf{x}), \quad (29)$$

for $f(y, t, \mathbf{x})$, taking the derivative, and setting $\epsilon = 0$:

$$\begin{aligned} \phi(Z, \mathcal{P}) &= \int yf(y|t, \mathbf{x})f(\mathbf{x}) \left[\frac{\delta_{\tilde{y}, \tilde{t}, \tilde{\mathbf{x}}}(y, t, \mathbf{x})}{f(y, t, \mathbf{x})} \right. \\ &\quad \left. + \frac{\delta_{\tilde{\mathbf{x}}}(\mathbf{x})}{f(\mathbf{x})} - \frac{\delta_{\tilde{t}, \tilde{\mathbf{x}}}(t, \mathbf{x})}{f(t, \mathbf{x})} - 1 \right] dyd\mathbf{x}, \end{aligned} \quad (30)$$

$$\begin{aligned}
\phi(Z, \mathcal{P}) &= \int \frac{yf(y|t, \mathbf{x})f(\mathbf{x})\delta_{\tilde{y}, \tilde{t}, \tilde{\mathbf{x}}}(y, t, \mathbf{x})}{f(y|t, \mathbf{x})f(t|\mathbf{x})f(\mathbf{x})} dyd\mathbf{x} \\
&\quad + \int \frac{yf(y|t, \mathbf{x})f(\mathbf{x})\delta_{\tilde{\mathbf{x}}}(\mathbf{x})}{f(\mathbf{x})} dyd\mathbf{x} \\
&\quad - \int \frac{yf(y|t, \mathbf{x})f(\mathbf{x})\delta_{\tilde{t}, \tilde{\mathbf{x}}}(t, \mathbf{x})}{f(t|\mathbf{x})f(\mathbf{x})} dyd\mathbf{x} \\
&\quad - \int yf(y|t, \mathbf{x})f(\mathbf{x}) dyd\mathbf{x},
\end{aligned} \tag{31}$$

$$\begin{aligned}
\phi(Z, \mathcal{P}) &= \delta_{\tilde{t}}(t) \int \frac{y\delta_{\tilde{y}}(y)}{f(t|\tilde{\mathbf{x}})} dy + \int yf(y|t, \tilde{\mathbf{x}}) dy \\
&\quad - \delta(t) \int \frac{yf(y|t, \tilde{\mathbf{x}})}{f(t|\tilde{\mathbf{x}})} dy - \Psi(\mathcal{P}) \\
&= \frac{\delta_{\tilde{t}}(t)}{f(t|\tilde{\mathbf{x}})} (\tilde{y} - \mathbb{E}[y|t, \tilde{\mathbf{x}}]) + \mathbb{E}[y|t, \tilde{\mathbf{x}}] - \Psi(\mathcal{P}),
\end{aligned} \tag{32}$$

$$\phi(Z, \mathcal{P}) = \frac{\delta_{\tilde{t}}(t)}{f(t|\tilde{\mathbf{x}})} (\tilde{y} - \mathbb{E}[y|t, \tilde{\mathbf{x}}]) + \mathbb{E}[y|t, \tilde{\mathbf{x}}] - \Psi(\mathcal{P}). \tag{33}$$

Once again, in order to evaluate this we need to evaluate it at $\hat{\mathcal{P}}_n$, and we also need plug-in estimators $\pi(\tilde{\mathbf{x}}) \approx f(t|\tilde{\mathbf{x}})$ (propensity score model), and $m(t, \tilde{\mathbf{x}}) \approx \mathbb{E}[Y|t, \tilde{\mathbf{x}}]$ (outcome model). The propensity score model represents a nuisance parameter and contributes to bias. This finally results in:

$$\phi(Z, \hat{\mathcal{P}}_n) = \frac{\delta_{\tilde{t}}(t)}{\pi(\tilde{\mathbf{x}})} (\tilde{y} - m(t, \tilde{\mathbf{x}})) + m(t, \tilde{\mathbf{x}}) - \Psi(\mathcal{P}). \tag{34}$$

C.2. Statistical Inference with Influence Functions

Following [65, p.75] we can derive 95% confidence intervals from the influence function as follows (assuming normal distribution):

$$\begin{aligned}
\widehat{\text{Var}}(\phi) &= \frac{1}{n} \sum_i^n \left[\phi(Z_i) - \frac{1}{n} \sum_j^n \phi(Z_j) \right]^2, \\
\widehat{\text{se}} &= \sqrt{\frac{\widehat{\text{Var}}(\phi)}{n}}, \\
\Psi^*(\hat{\mathcal{P}}_n) &\pm 1.96 \frac{\widehat{\text{se}}}{\sqrt{n}}, \\
p_{\text{val}} &= 2 \left[1 - \Phi \left(\left| \frac{\Psi^*(\hat{\mathcal{P}}_n)}{\widehat{\text{se}}/\sqrt{n}} \right| \right) \right],
\end{aligned} \tag{35}$$

where $\Psi^*(\hat{\mathcal{P}}_n)$ is the estimated target quantity after bias correction has been applied, Φ is the CDF of a normal distribution, $\widehat{\text{se}}$ is the sample standard error, and p_{val} is the p -value.

D. General Graphical Models

Throughout this paper, we focused on the estimation of average treatment effect in the setting of Figure 2. However, the methods discussed in this paper can be applied for more complex estimands with an arbitrary causal graph structure, as long as the estimand at hand is causally *identifiable* from the observed data. In this section, we discuss the derivation of influence functions for a general form of an estimand in a general graphical model.

D.1. Influence Function of an Interventional Distribution

Causal identification of interventional distributions is well-studied in the literature. In the case of full observability, any interventional distribution is identifiable using (extended) g-formula [16, 53]. If some variables of the causal system are unobserved, all interventional distributions are not necessarily identifiable. Tian and Pearl [61] provided necessary and sufficient conditions of identifiability in such models. Causal identification problem in DAGs with unobserved (latent) variables can equivalently be defined on *acyclic directed mixed graphs* (ADMGs) which represent the DAGs that share the same identification functionals [15, 50, 51]. ADMGs are acyclic mixed graphs with directed and bidirected edges, that result from a DAG through a latent projection operation onto a graph over the observable variables [69].

Pearl's do-calculus is shown to be complete for the identification of interventional distributions [31]. Let \mathbf{V} denote the set of all observed variables. Starting with an identifiable interventional distribution $P(\mathbf{y}|do(\mathbf{T} = \mathbf{t}^*))$, an identification functional of the following form is derived using do-calculus:

$$P(\mathbf{y}|do(\mathbf{T} = \mathbf{t}^*)) = \sum_{\mathbf{s}} \frac{\prod_i \mathcal{P}(\mathbf{a}_i|\mathbf{b}_i)}{\prod_j \mathcal{P}(\mathbf{c}_j|\mathbf{d}_j)}, \tag{36}$$

where $\mathbf{a}_i, \mathbf{b}_i, \mathbf{c}_j$, and \mathbf{d}_j are realizations of $\mathbf{A}_i, \mathbf{B}_i, \mathbf{C}_j$, and \mathbf{D}_j , respectively, and $\mathbf{A}_i, \mathbf{B}_i, \mathbf{C}_j, \mathbf{D}_j, \mathbf{S}$ are subsets of variables such that for each i and j , $\mathbf{A}_i \cap \mathbf{B}_i = \emptyset$ and $\mathbf{C}_j \cap \mathbf{D}_j = \emptyset$. Note that the sets \mathbf{B}_i and \mathbf{D}_j might be empty. The $\sum_{\mathbf{s}}$ symbol in Equation (36) indicates a summation over the values of the set of variables \mathbf{S} in the discrete case, and an integration over these values in the continuous setting. To derive the influence function of Eq. (36), we begin with a conditional distribution of the form $\mathcal{P}(\mathbf{a}|\mathbf{b})$. If $\mathbf{b} \neq \emptyset$, we can write

$$\begin{aligned}
\mathcal{P}_\epsilon(\mathbf{v}) &= (1 - \epsilon)\mathcal{P}(\mathbf{v}) + \epsilon\delta_{\tilde{\mathbf{v}}}(\cdot), \\
\mathcal{P}_\epsilon(\mathbf{a}|\mathbf{b}) &= \frac{\mathcal{P}_\epsilon(\mathbf{a}, \mathbf{b})}{\mathcal{P}_\epsilon(\mathbf{b})}, \\
\left. \frac{d\mathcal{P}_\epsilon(\mathbf{a}|\mathbf{b})}{d\epsilon} \right|_{\epsilon=0} &= \frac{\delta_{\tilde{\mathbf{a}}, \tilde{\mathbf{b}}}(\mathbf{a}, \mathbf{b}) - \mathcal{P}(\mathbf{a}, \mathbf{b})}{\mathcal{P}(\mathbf{b})} \\
&\quad - \frac{\mathcal{P}(\mathbf{a}, \mathbf{b})[\delta_{\tilde{\mathbf{b}}}(\mathbf{b}) - \mathcal{P}(\mathbf{b})]}{\mathcal{P}^2(\mathbf{b})} \\
&= \mathcal{P}(\mathbf{a}|\mathbf{b}) \cdot \left(\frac{\delta_{\tilde{\mathbf{a}}, \tilde{\mathbf{b}}}(\mathbf{a}, \mathbf{b})}{\mathcal{P}(\mathbf{a}, \mathbf{b})} - \frac{\delta_{\tilde{\mathbf{b}}}(\mathbf{b})}{\mathcal{P}(\mathbf{b})} \right),
\end{aligned} \tag{37}$$

where $\tilde{\mathbf{v}}$ is the point that we compute the influence function at, and $\tilde{\mathbf{a}}, \tilde{\mathbf{b}}$ are the values of sets of variables $\mathbf{A}, \mathbf{B} \subseteq \mathbf{V}$ that are consistent with $\tilde{\mathbf{v}}$. For an empty \mathbf{b} , using similar arguments, we have:

$$\left. \frac{d\mathcal{P}_\epsilon(\mathbf{a})}{d\epsilon} \right|_{\epsilon=0} = \mathcal{P}(\mathbf{a}) \cdot \left(\frac{\delta_{\tilde{\mathbf{a}}}(\mathbf{a})}{\mathcal{P}(\mathbf{a})} - 1 \right). \tag{38}$$

With slight abuse of notation, for $\mathbf{b} = \emptyset$, we define $\frac{\delta_{\tilde{\mathbf{b}}}(\mathbf{b})}{\mathcal{P}(\mathbf{b})} = 1$. Using Eq. (37) and Eq. (38), we can now derive the influence function of Eq. (36).

$$\begin{aligned}
\phi(\tilde{\mathbf{v}}, \mathcal{P}) &= \left. \frac{d((1 - \epsilon)\mathcal{P} + \epsilon\delta_{\tilde{\mathbf{v}}})}{d\epsilon} \right|_{\epsilon=0} = \\
&\quad \sum_{\mathbf{s}} \frac{\prod_i \mathcal{P}(\mathbf{a}_i|\mathbf{b}_i)}{\prod_j \mathcal{P}(\mathbf{c}_j|\mathbf{d}_j)} \cdot \left[\sum_i \left(\frac{\delta_{\tilde{\mathbf{a}}, \tilde{\mathbf{b}}_i}(\mathbf{a}_i, \mathbf{b}_i)}{\mathcal{P}(\mathbf{a}_i, \mathbf{b}_i)} - \frac{\delta_{\tilde{\mathbf{b}}_i}(\mathbf{b}_i)}{\mathcal{P}(\mathbf{b}_i)} \right) \right. \\
&\quad \left. - \sum_j \left(\frac{\delta_{\tilde{\mathbf{c}}, \tilde{\mathbf{d}}_j}(\mathbf{c}_j, \mathbf{d}_j)}{\mathcal{P}(\mathbf{c}_j, \mathbf{d}_j)} - \frac{\delta_{\tilde{\mathbf{d}}_j}(\mathbf{d}_j)}{\mathcal{P}(\mathbf{d}_j)} \right) \right].
\end{aligned} \tag{39}$$

Note that we used $\frac{d}{d\epsilon} \frac{1}{\mathcal{P}_\epsilon(\mathbf{c}|\mathbf{d})} = -\frac{\frac{d}{d\epsilon} \mathcal{P}_\epsilon(\mathbf{c}|\mathbf{d})}{\mathcal{P}_\epsilon^2(\mathbf{c}|\mathbf{d})}$. Equation (39) is the foundation to the approach that shall be discussed in the following section for deriving the influence function of a general class of estimands.

D.2. Influence Function of a General Estimand

We have so far discussed the influence function of a causal effect of the form $\mathcal{P}(y|do(\mathbf{T} = \mathbf{t}^*))$. In this section, we show how IFs can be derived for any general estimand of the form:

$$\Psi(\mathcal{P}) = \mathbb{E}_{\mathcal{P}}[\kappa(\mathcal{P})], \tag{40}$$

where $\kappa(\cdot)$ is a functional. Then we have:

$$\begin{aligned}
\mathcal{P}_\epsilon &= \epsilon\hat{\mathcal{P}}_n + (1 - \epsilon)\mathcal{P}, \\
\Psi(\mathcal{P}_\epsilon) &= \int \kappa(\mathcal{P}_\epsilon)\mathcal{P}_\epsilon d\mathbf{v}, \\
\left. \frac{d\Psi(\mathcal{P}_\epsilon)}{d\epsilon} \right|_{\epsilon=0} &= \\
&\quad \int \left(\frac{d\mathcal{P}_\epsilon}{d\epsilon} \cdot \kappa(\mathcal{P}_\epsilon) + \frac{d\kappa}{d\mathcal{P}} \cdot \frac{d\mathcal{P}_\epsilon}{d\epsilon} \cdot \mathcal{P}_\epsilon \right) \Big|_{\epsilon=0} d\mathbf{v} \\
&= \int \left(\kappa(\mathcal{P}) + \frac{d\kappa}{d\mathcal{P}} \cdot \mathcal{P} \right) \cdot \left. \frac{d\mathcal{P}_\epsilon}{d\epsilon} \right|_{\epsilon=0} d\mathbf{v} \\
&= \int \kappa(\mathcal{P}) \cdot \left. \frac{d\mathcal{P}_\epsilon}{d\epsilon} \right|_{\epsilon=0} d\mathbf{v} + \mathbb{E}_{\mathcal{P}} \left[\left. \frac{d\kappa}{d\mathcal{P}} \cdot \frac{d\mathcal{P}_\epsilon}{d\epsilon} \right|_{\epsilon=0} \right].
\end{aligned} \tag{41}$$

The value of $\left. \frac{d\mathcal{P}_\epsilon}{d\epsilon} \right|_{\epsilon=0}$ can be plugged into Eq. (41) using Eq. (39) and Eq. (20), which completes the derivation of the IF for the estimand in Eq. (40). As an example, if the queried estimand is the average density of a variable Y , that is, κ is the identity functional, then:

$$\begin{aligned}
\Psi(\mathcal{P}) &= \int \mathcal{P}^2(y) dy, \\
\left. \frac{d\Psi(\mathcal{P}_\epsilon)}{d\epsilon} \right|_{\epsilon=0} &= \int (\mathcal{P} + 1 \cdot \mathcal{P}) \cdot \left. \frac{d\mathcal{P}_\epsilon}{d\epsilon} \right|_{\epsilon=0} dy \\
&= \int 2\mathcal{P}(y) \cdot \left. \frac{d\mathcal{P}_\epsilon}{d\epsilon} \right|_{\epsilon=0} dy.
\end{aligned}$$

Algorithm (1) summarises the steps of our proposed automated approach to derive the influence function of an estimand of the form presented in Eq. (40), given a general graphical model. Note that if the effect is identifiable, this algorithm outputs the analytic influence function, and otherwise, throws a failure. A demonstrative example can be found in the associated code repository in the form of a notebook, and/or in the attached supplementary code.

Algorithm 1 IF of an identifiable effect.

- input:** An estimand $\Psi(\mathcal{P})$ of the form of Eq. (40), an interventional distribution \mathcal{P} , causal graph \mathcal{G}
 - output:** The analytic IF of $\Psi(\mathcal{P})$ if \mathcal{P} is identifiable, fail o.w.
 - 1: **if** \mathcal{P} is identifiable **then**
 - 2: $\tilde{\mathcal{P}} \leftarrow$ the identification functional of \mathcal{P} (Eq. (36))
using do-calculus
 - 3: $\phi \leftarrow$ the IF of \mathcal{P} as in Eq. (39)
 - 4: $\left. \frac{d\Psi(\mathcal{P}_\epsilon)}{d\epsilon} \right|_{\epsilon=0} \leftarrow$ the formulation as in Eq. (41)
 - 5: $\Phi \leftarrow$ Plug ϕ into $\left. \frac{d\Psi(\mathcal{P}_\epsilon)}{d\epsilon} \right|_{\epsilon=0}$ using Eq. (20)
 - 6: **return** Φ
 - 7: **else**
 - 8: **return** FAIL
-

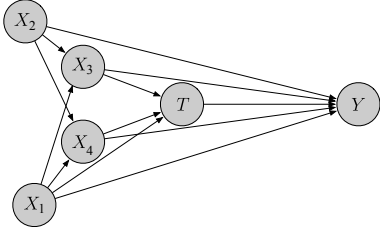


Figure 3. Graph for the ‘LF’ dataset used in [43].

E. Data

In this part of the supplementary material we provide details about the datasets used in the evaluations.

E.1. LF Dataset Variants

The graph for the synthetic ‘LF’ dataset used in [43] is given in Fig. 3. The DGP is based on a model for cancer patient outcomes for patients treated with monotherapy ($t = 1$) and dual therapy ($t = 0$) and the generating equations are as follows:

$$\begin{aligned}
 X_1 &\sim Be(0.5), & X_2 &\sim Be(0.65) \\
 X_3 &\sim \text{int}[U(0, 4)], & X_4 &\sim \text{int}[U(0, 5)] \\
 T &\sim Be(p_T), \text{ where} \\
 p_T &= \sigma(-5 + 0.05X_2 + 0.25X_3 + 0.6X_4 + 0.4X_2X_4) \\
 Y_1 &= \sigma(-1 + 1 - 0.1X_1 + 0.35X_2 \\
 &\quad + 0.25X_3 + 0.2X_4 + 0.15X_2X_4) \\
 Y_0 &= \sigma(-1 + 0 - 0.1X_1 + 0.35X_2 \\
 &\quad + 0.25X_3 + 0.2X_4 + 0.15X_2X_4)
 \end{aligned} \tag{42}$$

where $\text{int}[\cdot]$ is an operator which rounds the sample to the nearest integer, Be is a Bernoulli distribution, U is a uniform distribution, σ is the sigmoid function, and Y_1 and Y_0 are the counterfactual outcomes when $T = 1$ and $T = 0$, respectively. Covariate X_1 represents biological sex, X_2 represents age category, X_3 represents cancer stage, and X_4 represents comorbidities.

We create a variant (v2) of this DGP by introducing non-linearity into the outcome, and then into the treatment assignment as follows:

$$Y_1 = \sigma(\exp[-1 + 1 - 0.1X_1 + 0.35X_2 + 0.25X_3 + 0.2X_4 + 0.15X_2X_4]) \tag{43}$$

The two variants are designed to yield near positivity violations in order to highlight weaknesses in methods which depend on a reliable propensity score model. Figures 4 and 5 provide information on the propensity scores for the v1 and v2 variants (v2 has the same propensity score generating model as v1).

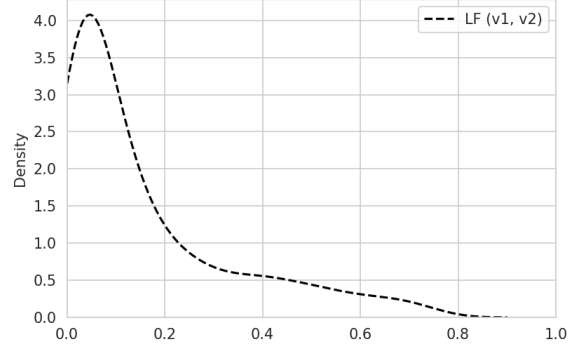


Figure 4. Marginal propensity scores for the LF (v1) and LF (v2) datasets. Note that the minimum probability of treatment in a random draw from the DGP is 0.007. The datasets are intentionally designed such that certain subgroups are unlikely to receive treatment, resulting in near-positivity violations.

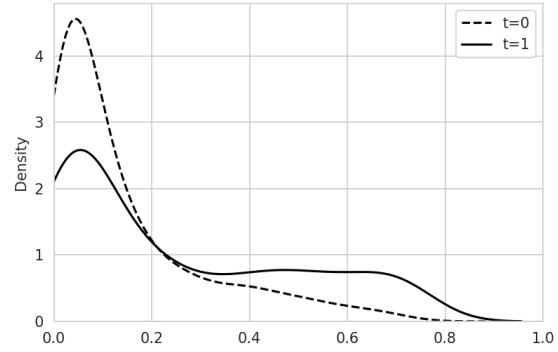


Figure 5. Propensity scores by treatment assignment for a sample from the LF (v1) dataset.

E.2. IHDP

The IHDP⁷ dataset corresponds with usual setting A of the NPCI data generating package [13] (see [56, 58, 77]) and comprises 608 untreated and 139 treated samples (747 in total). This variant actually corresponds with variant B in [27]. There are 25 covariates, 19 of which are discrete/binary, and the rest are continuous. The outcome generating process is designed such that under treatment, the potential outcome is exponential, whereas under no treatment the outcome is a linear function of the covariates [11].

F. CFR and MultiNet Hyperparameter Search

For the neural network methods, we undertake 15 trials on a train/test split for each of the 100 samples from the

⁷Available from <https://www.fredjo.com/>

Table 2. Hyperparameter search space for neural network based methods.

Parameter	Min	Max
Batch size	10	64
L2 Weight Penalty	1e-5	1e-3
No. of Iterations	2000	10000
Learning Rate	1e-5	1e-2
No. Layers	4	14
Dropout Prob.	0.1	0.5
No. Neurons per Layer	5	200

DGP. Distinct hyperparameter searches are undertaken for methods using targeted regularization. The hyperparameters which are included in the search space are present in Table 2. Note that the iteration count is not in terms of epochs - it represents the number of batches sampled randomly from the dataset. The number of iterations can be multiplied by the batch size and divided by the dataset size to approximately determine the equivalent number of epochs this represents.

G. Complete Results and Further Discussion

Table 3 provides the complete set of tabulated results, whilst Figures 6, 7, and 8 provide probability plots for the LF (v1), LF (v2), and IDHP datasets. The figures include an indication of the sample mean as well as the sample mode. The mode is important to consider in cases where the distribution may be non-Gaussian (and indeed, this is one of the criteria we test for). We estimate the mode using a Gaussian kernel density estimation method with the Scipy simplicial homology global optimization algorithm [14, 33]. This algorithm is used to identify the point which minimizes the reciprocal of the log-likelihood under the estimated density.

G.1. Combining Targeted Regularization with Super Learner

As discussed in the main paper, targeted regularization was not found to consistently improve estimation, and further work is required to understand how its performance can be improved. However, we explored two further variants: ‘Treg w/ SL’ which uses a Super Learner (SL) as the propensity score model for computation of the clever covariate in the regularizer; and ‘Treg+submod w/ SL’ which is the same as ‘Treg w/ SL’ except that an additional submodel update step is performed once the neural network has been trained. In some cases both techniques worked, but their performance was also not consistent. For example, MN-Inc benefited from Treg+submod w/ SL on all three datasets, but did not perform as well as the highlighted (bold or underlined) alternatives. Hence, given the additional computational complexity of targeted regularization with or without a subsequent update step, and with or with-

out a SL propensity score model, the results make it difficult to argue for these approaches.

G.2. Probability Plots

As mentioned above, the probability plots provide a visual means to assess normality and, in particular, whether the mode of the distribution of estimates differs from the mean. In the interests of brevity, we focus our discussion on the notable results for the LF (v1) and LF (v2) datasets. As noted in [11], the IHDP dataset exhibits some characteristics which may preferentially bias certain estimators, and we refrain from providing commentary on these results, but nonetheless present the associated probability plots in Figure 8 for interested readers.

LF (v1) in Figure 6: The notable results for this dataset were Logistic Regression (LR), LR with a onestep update, base CFR, CFR with a onestep update, and MN-Inc with a onestep update.

If we begin by considering the plot for LR Figure 6 (top row, 2nd column), we see a good clustering of mean, mode, and true ATE (green, blue, and dashed lines, respectively). Note, however, that there is some deviation from normality, particularly at the upped tail of the distribution in probability plot, where the estimates diverge from normality. An improvement can be witnessed in the graph for LF+onestep (top row, 3rd column), where the mean, mode, and true ATE are even more tightly clustered. One can conclude from this that LR with a onestep update is a good model for these data. In contrast, whilst CFR base (2nd row, 1st column) has a mode that overlays well on top of the true (dashed) population ATE, the mode (blue line) of the distribution of estimates falls far from the mean (green line). Alternatively, the CFR+onestep (2nd row, 2nd column) exhibits a different problem - the mean and mode overlay each other, but both fall far from the true ATE. This suggests that whilst the MSE was improved by the onestep update, the mode was actually worsened, even though it coincided with the mean. These behaviours highlight how important it is to consider multiple metrics and statistics for evaluating the efficacy of these methods. In contrast with the CFR variants, MN-Inc+onestep (3rd row, 4th column) demonstrates excellent behaviour - the mean, mode, and true ATE are all overlaying each other, and the estimates are tightly grouped along the diagonal line, thereby exhibiting normality.

LF (v2) in Figure 7: Consider LR, LR+onestep, base CFR, CFR+onestep, CFR+onestep w/SL, and MN-Inc+onestep, we see similar but more extreme behaviour in the probability plots for LF (v2) than in LF (v1). This dataset introduced an exponential non-linearity into the outcome model. In the probability plot for LR (top row, 2nd column), we see that the mean and mode of the estimates is offset from the true ATE. However, the onestep update is able to rescue this estimator, and the plot for LR+onestep

(top row, 2nd column) demonstrates the double-robustness property. In this case, the propensity score model was ‘good enough’ to make up for the misspecification of the outcome model, and the LR+onestep result is much improved. In stark contrast, the CFR base result (2nd row 1st column) is poor - whilst the mode (blue line) is close to the true ATE (dashed line), the estimates are highly non-normally distributed and have a high standard error. The results for CFR+onestep demonstrate how the update step does not work to fix the issue.

However, the CFR+onestep w/ SL utilizes a SL propensity score model, and once again we witness the power of the double-robustness property to compensate for the misspecification of the outcome model - the mean, mode, and true ATE are all overlays of each other. MN-Inc+onestep demonstrates similar but much less extreme issues to CFR+onestep, and here the use of the SL propensity score model fixed the residual misspecification of the model.

G.3. Summary

The probability plots once again highlight the potential for influence functions to ‘rescue’ poor estimators, improving estimation, tightening confidence intervals, and yielding normal distributions of estimates.

H. Things that Did Not Work

One of the initial possibilities that we considered which might explain why the neural network methods were not performing as well as the logistic regressor or the Super Learner on the least complex dataset (with only one quadratic feature), was that the calibration of the networks might be poor [22]. However, we tried calibrating the trained outcome and treatment model networks using temperature scaling. We found it to be unsuccessful, and we leave an exploration of why it failed to future work.

Additionally, we tried only performing hyperparameter search with a held-out test set *once* at the beginning of the 100 subsequent simulations for each model and dataset variant, rather than performing it for every single simulation. This did not work, and we found that if the first network ‘designed’ through hyperparameter search happened to be degenerate with respect to its performance as a plug-in estimator (notwithstanding its potentially adequate performance as an outcome model), then it will be degenerate for all simulations, and yield incredibly biased results. However, performing hyperparameter search for every simulation more accurately represents the use of these algorithms in practice.

This problem also highlights the importance of fitting multiple neural networks on the same data. As supervision is not available, the usual metrics for hyperparameter search (based on *e.g.*, held out data loss scores) can be a poor indicator for the efficacy of the network as a plug-in estimator.

By re-performing hyperparameter search, even on the same data (put perhaps, with different splits), one can effectively bootstrap to average out the variability associated with the hyperparameter search itself. Indeed, as the results show, the average estimates for the ATE using CFR net are close to the true ATE, even if the variance of the estimation is relatively high. We leave a comparison of the contribution of variance from hyperparameter search to further work.

Table 3. Mean squared errors (MSE) and standard error (s.e.) (lower is better) and p -values from a Shapiro-Wilks test for normality (higher is better) for 100 simulations. **Bold** indicates best result for each algorithm, **bold and underline** indicates best result for each dataset variant. The best results are those judged to yield *both* normally distributed estimation ($p > 0.05$), as well as low mean squared error. **Base** indicates the associated algorithm is being used as an outcome model, which is ‘plugged in’ to the ATE estimating equation. **Onestep** indicates that a propensity score model has been fit using the same algorithm, and the onestep update has been applied. **Submod** also indicates a propensity score model has been fit using the same algorithm, but now a targeted submodel approach has been used. **Treg** indicate that the (neural network) approach uses targeted regularization during the training process, where the associated propensity score model is fit using a different instance of the same network. **Treg+submod** indicates that targeted regularization has been used during the training of the neural network, and then once the training is complete, a targeted submodel update has been performed on top of this. **Onestep w/ SL** indicates that a onestep update has been performed, where the propensity score is modelled using a Super Learner (SL). **Treg w/ SL** indicates that targeted regularization has been applied during training, but the associated propensity score is modelled using a SL. **Treg + Submod w/SL** Indicates that both targeted learning as well as subsequent submodel update step has been used, where, for both the regularization and the submodel, the propensity score has been modelled using a SL.

Dataset	Algorithm	Base		Onestep		Submod		Treg		Treg+Submod		Onestep w/ SL		Submod w/ SL		Treg w/ SL		Treg+Submod w/ SL							
		p	s.e.	p	s.e.	p	s.e.	p	s.e.	p	s.e.	p	s.e.	p	s.e.	p	s.e.	p	s.e.						
n=5000	LR	.001	.0004	.002	.276	.007	.003	.248	.0008	.003	.008	.003	.378	.0006	.003	.591	.0008	.003	.024	.0094	.008	.498	.0016	.003	
	SL	.001	.0004	.002	.53	.0008	.003	.651	.0009	.003	.008	.003	.396	.0006	.003	.909	.0015	.003	.024	.0094	.008	.498	.0016	.003	
	CFR	.052	.0008	.003	.001	.0042	.004	.01	.01	.003	.07	.0113	.008	.0	.0105	.002	.681	.001	.003	.0013	.004	.386	.0009	.003	
	MN-Inc	.135	.0009	.003	.78	.0007	.003	.394	.001	.003	.729	.0012	.003	.639	.0008	.003	.329	.001	.003	.0013	.004	.391	.0011	.003	
	MN-Inc+LM	.053	.0018	.004	.231	.0014	.002	.0	.0018	.003	.083	.0086	.007	.702	.0045	.004	.831	.0007	.003	.011	.0096	.008	.714	.0012	.003
	MN-Casc+LM	.066	.0024	.002	.752	.0007	.003	.204	.0037	.003	.0	.0091	.008	.74	.0036	.003	.625	.001	.003	.0	.0082	.008	.964	.0011	.003
n = 5000	LR	.066	.0024	.002	.752	.0007	.003	.497	.0008	.003	.0	.0091	.008	.74	.0036	.003	.625	.001	.003	.0	.0082	.008	.964	.0011	.003
	SL	.349	.0017	.003	.938	.0008	.003	.92	.0009	.003	.0	.008	.0162	.002	.002	.065	.0015	.003	.0	.0354	.012	.207	.0016	.003	
	CFR	.119	.001	.003	.204	.0006	.003	.211	.0008	.003	.002	.0009	.002	.029	.0008	.003	.678	.0026	.003	.002	.001	.002	.013	.0009	.003
	MN-Inc	.0	.0011	.003	.438	.0009	.003	.813	.0011	.003	.139	.0071	.005	.678	.0026	.003	.959	.0005	.002	.002	.0015	.006	.905	.0011	.003
	MN-Inc+LM	.0	.002	.004	.013	.0033	.002	.892	.0043	.003	.77	.014	.006	.365	.0101	.002	.272	.0007	.003	.025	.0165	.006	.759	.0014	.003
	MN-Casc	.257	.0113	.007	.349	.0032	.003	.001	.0083	.002	.066	.0295	.007	.0	.0112	.002	.897	.0006	.003	.335	.0332	.007	.483	.0015	.003
IHDP	LR	.022	.1818	.019	.0	.0576	.035	.0	.0461	.044	.0	.0	.1322	.019	.0	.0597	.03	.0	.0	.0	.0	.0	.0	.0	.0
	SL	.0	.0466	.032	.0	.2865	.074	.0	.0346	.034	.0	.0	.0	.0	.0	.0	.0	.0	.0	.0	.0	.0	.0	.0	.0
	CFR	.0	.7709	.098	.0	.0297	.004	.0	.0439	.052	.0	.25.5	.3	.0	.0604	.051	.0	.2626	.063	.0	.109	.255	.0	.63	.173
	MN-Inc	.0	.0324	.042	.0	.0259	.004	.0	.8.7	.299	.0	.0482	.042	.0	.30.8	.537	.0	.0243	.044	.0	.0506	.042	.0	.0293	.045
	MN-Inc+LM	.0	.0393	.045	.0	.0259	.004	.0	.9849	.099	.0	.1332	.038	.0	.1.9	.138	.0	.0243	.044	.0	.1348	.039	.0	.0366	.043
	MN-Casc	.0	.1977	.046	.0	.0737	.04	.0	.064	.04	.0	.2.9	.115	.0	.102	.042	.0	.0816	.042	.0	.2.7	.011	.0	1.3	.099
n = 747	MN-Casc+LM	.0	4.7	.158	.0	1.4	.093	.0	.2118	.049	.0	.23.9	.164	.0	.1824	.06	.0	1.1	.079	.0	24.6	.163	.0	35.8	.268

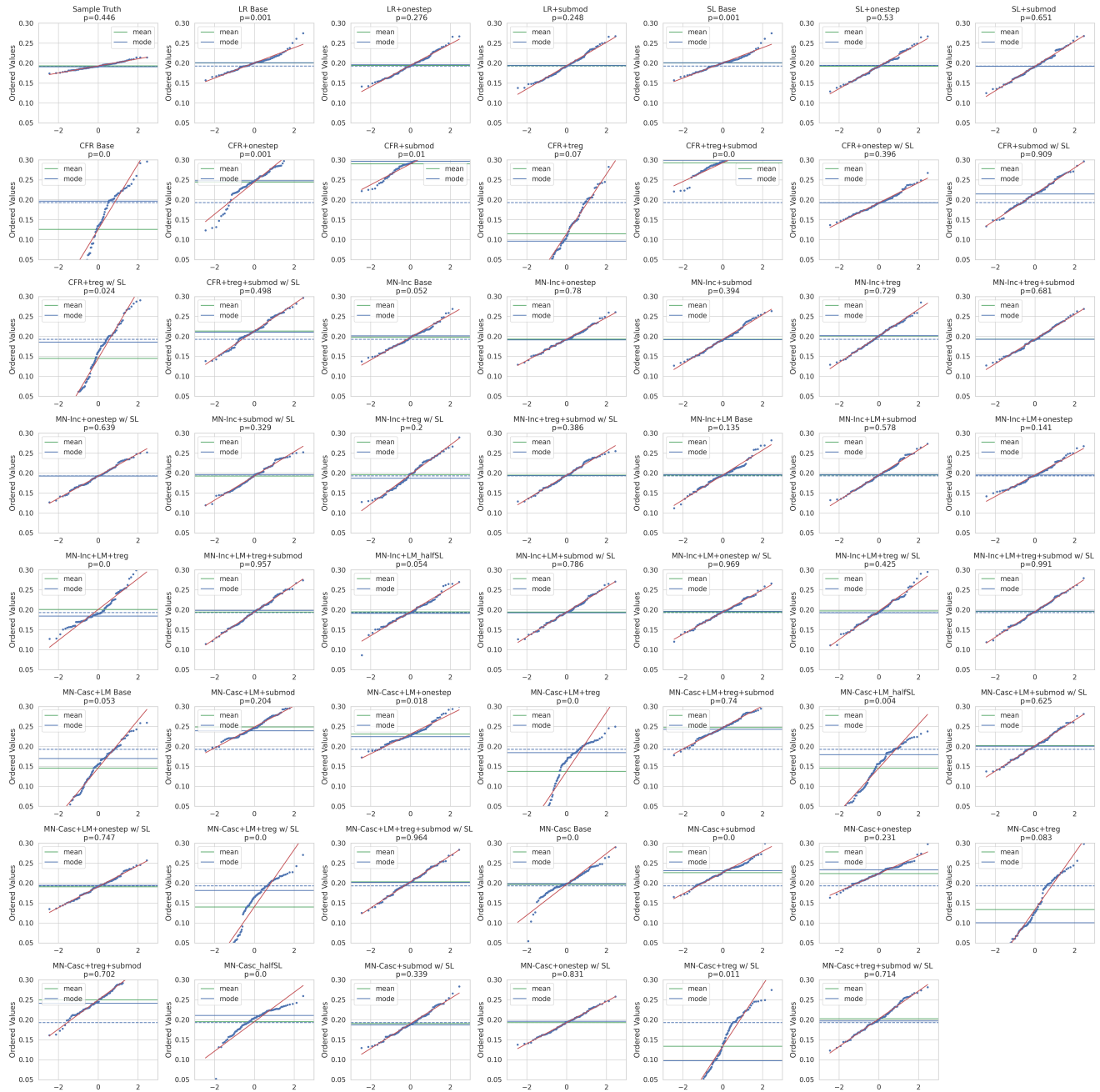


Figure 6. Probability plots for 100 simulations of the different methods on the LF (v1) dataset with $n = 5000$. Dashed horizontal line indicates true population-level ATE.



Figure 7. Probability plots for 100 simulations of the different methods on the LF (v2) dataset with $n = 5000$.

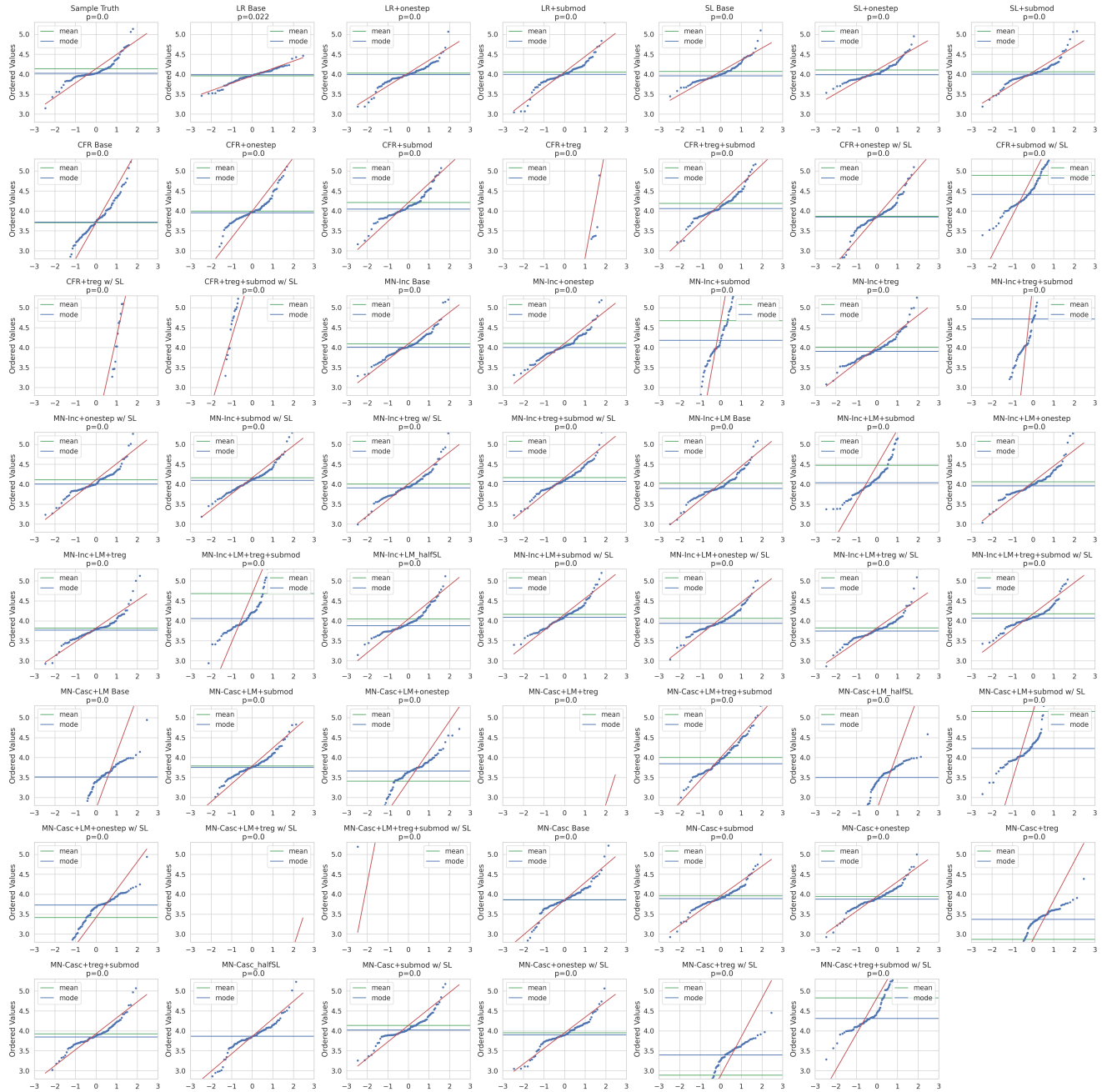


Figure 8. Probability plots for 100 simulations of the different methods on the IHDP dataset with $n = 747$.